[Electronic Supplementary Information to accompany:]

Improved anti-proliferative effect of doxorubicin-containing polymer nanoparticles upon surface modification with cationic groups

Sai Archana Krovi,[a] Elden P. Swindell,[b] Thomas V. O'Halloran,[a] and SonBinh T. Nguyen[a]*

[a]*Department of Chemistry and Chemistry of Life Processes Institute, Northwestern University, 2145 Sheridan Road, Evanston, Illinois 60208-3113, USA.*

[b]*Department of Chemical and Biological Engineering, Northwestern University, 2145 Sheridan Road, Evanston, Illinois 60208, USA.*

Table of Contents *Page number*

I. General information.

All synthetic manipulations were performed under a dry nitrogen atmosphere using either standard Schlenk techniques or an inert-atmosphere glovebox, unless otherwise noted. HPLC-grade dichloromethane (DCM), methanol (MeOH), and dimethylformamide (DMF) were dried over neutral alumina *via* the Dow-Grubbs solvent system[S1] installed by Glass Contours (now JC Meyer Solvent Systems, Laguna Beach, CA, USA). Solvents were collected under argon, degassed under vacuum, and stored under nitrogen in a Strauss flask prior to use. All flash chromatography was carried out using a 56-mm inner diameter column containing 150-mm length of silica gel under a positive pressure of laboratory air.

^{1}H and ^{13}C NMR spectra were recorded on a Bruker 500 FT-NMR spectrometer (500 MHz for ^{1}H NMR, 125 MHz for ^{13}C NMR). ^{1}H NMR data are reported as follows: chemical shift (multiplicity (b = broad, s = singlet, d = doublet, t = triplet, q = quartet, qn = quintet, and m = multiplet) and peak assignments). ^{1}H and ^{13}C chemical shifts are reported in ppm downfield from tetramethylsilane (TMS). Electrospray-ionization mass spectrometric (ESIMS) data was obtained on a Micromass Quattro II Triple Quadrupole mass spectrometer (Micromass, Inc., Beverly, MA, USA). UV-vis absorption spectra for all samples were obtained on a CARY 300 Bio UV-vis spectrometer (Varian, Inc., Cary, NC, USA).

Polymer molecular weights relative to polystyrene standards were measured on a Waters gel-permeation chromatograph (GPC, Waters Corp., Milford, MA, USA) equipped with Breeze software, a 717 autosampler, Shodex KF-G guard column, KF-803L and KF-806L columns in series, a Waters 2440 UV detector, and a 410 RI

detector. HPLC-grade THF was used as the eluent at a flow rate of 1.0 mL/min and the instrument was calibrated using polystyrene standards (Aldrich, 15 standards, 760-1,800,000 Daltons). Molecular-weight data are reported after being rounded off to the nearest 1K Dalton.

Transmission electron microscopy (TEM) was performed on a Hitachi HF8100 microscope (Hitachi High Technologies America, Schaumburg, IL, USA) operating at an accelerating voltage of 200 kV. For the observation of the size and distribution of the polymer nanoparticles (PNPs) prepared in ultrapure deionized water, colloidal samples (5 μL) were deposited from aqueous dispersions of the copolymer nanoparticles onto copper EM grids (400 mesh, Formvar/carbon-coated). The grids were allowed to air-dry at atmospheric pressure and room temperature before TEM measurements.

Dynamic light-scattering (DLS) measurements were performed on a Zetasizer Nano ZS (Malvern Instruments, Malvern, UK) with a He-Ne laser (633 nm). Non-invasive backscatter method (detection at 173° scattering angle) was used. The hydrodynamic diameters (D_H) and polydispersity indices (PDI) of polymer nanoparticles were calculated by the supplied instrument software (Zetasizer DTS).

An Eppendorf (Hauppauge, NY, USA) model 5804 R centrifuge was employed for centrifugation. All PNP surface modifications were performed using the platform shaker (Thermomixer R, Eppendorf, Hauppauge, NY, USA).

II. Materials.

Catalyst $(PCy_3)_2Cl_2Ru{=}CHPh$ (**5**) was purchased from Aldrich Chemicals Co. (Milwaukee, WI, USA) and used as received. Deuterated solvents were purchased from Cambridge Isotope Laboratories (Andover, MA, USA) and used without further purification, except for CD_2Cl_2 and $CDCl_3$, which were dried over calcium hydride, vacuum-transferred into an air-tight solvent bulb, and stored inside an inert-atmosphere glovebox before use.

All other reagents were purchased from Aldrich Chemicals Co. and used without further purification, unless otherwise noted. Ultrapure deionized water (18.2 MΩ·cm resistivity) was obtained from a Millipore Milli-Q Biocel A10 instrument (Millipore Inc., Billerica, MA, USA). Dialysis cassettes (MWCO = 3500) were purchased from Pierce Protein Research Products (Rockford, IL, USA). Formvar/Carbon, 400-mesh copper TEM grids were purchased from Ted Pella, Inc. (Redding, CA, USA).

III. Synthesis of monomer 4, block copolymer (2-*co*-4)$_{15}$-*b*-3$_{15}$, and the associated PNPs.

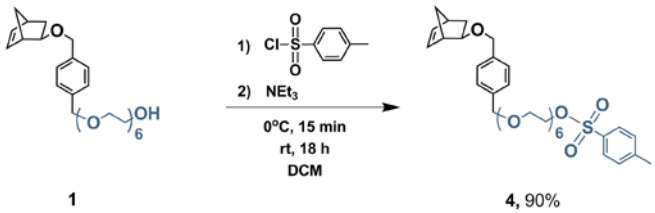

1 **4**, 90%

Synthesis of 1-[4-({bicyclo[2.2.1]hept-5-en-2-yloxy}methyl)phenyl]-2,5,8,11,14,17-hexaoxanonadecan-19-yl 4 methylbenzene-1-sulfonate (4). The following procedure was a modification of a previously published protocol.[S2] 4-toluenesulfonyl chloride (1.17 gm, 15.2 mmol) was added as a solid to a solution of 1-[4-({bicyclo[2.2.1]hept-5-en-2-yloxy}methyl)phenyl]-2,5,8,11,14,17-hexaoxanonadecan-19-ol (**1**, 150 mg, 0.303 mmol) in dry DCM (25 mL) in a 50-mL Schlenk flask. After the addition of triethylamine (0.93 mL, 6.67 mmol) using a gas-tight syringe, the

reaction mixture was allowed to stir for 15 min at 0 °C. The resulting solution was allowed to stir overnight at room temperature before being concentrated and purified by flash chromatography (95:5 v/v CH_2Cl_2:MeOH) to afford monomer **4** as a dark yellow oil (178 mg, 90% yield). ^{1}H NMR ($CDCl_3$, Fig. S1 (top)): δ 1.28-1.76 (m, 4H, 3- and 7-norbornenyl-H_2), 2.45 (s, 3H, aromatic-CH_3), 2.82 (b, 1H, 1-norbornenyl-*H*), 2.94 (b, 1H, 4-norbornenyl-*H*), 3.59-3.70 (m, 22H, OCH_2CH_2O), 4.19 (t, 2H, $CH_2CH_2OSO_2$), 4.45-4.56 (m, 5H, CH_2-C_6H_4-CH_2 and 2-norbornenyl-*H*), 5.89 (m, 1H, 6-norbornenyl-*H*), 6.18 (m, 1H, 5-norbornenyl-*H*), 7.32 (b, 4H, aromatic-*H*), 7.35 (d, 2H, aromatic-*H*), 7.81 (d, 2H, aromatic-*H*). ^{13}C NMR ($CDCl_3$, Fig. S1 (bottom)): δ 21.9 (*C*H_3), 34.5 (3-norbornenyl-*C*), 40.4 (4-norbornenyl-*C*), 46.1 (7-norbornenyl-*C*), 46.5 (1-norbornenyl-*C*), 68.9 ($CH_2CH_2OSO_2$), 69.4 (*C*$H_2CH_2OSO_2$), 70.7-70.9 (m, OCH_2CH_2O), 71.1 (CH-O-CH_2-Ph), 73.2 (Ph-O-CH_2-CH_2), 80.1 (2-norbornenyl-*C*), 127.6 (aromatic-*C*), 127.7 (aromatic-*C*), 129.2 (aromatic-*C*), 130.0 (aromatic-*C*), 133.2 (6-norbornenyl-*C*), 133.4 (aromatic-*C*), 137.4 (aromatic-*C*), 138.3 (aromatic-*C*), 140.7 (5-norbornenyl-*C*), 144.8 (aromatic-*C*). ESIMS (positive mode): *m/z* calculated for $C_{34}H_{48}O_{10}S$ $[M + Na]^+$: 648.789. Found: 648.801.

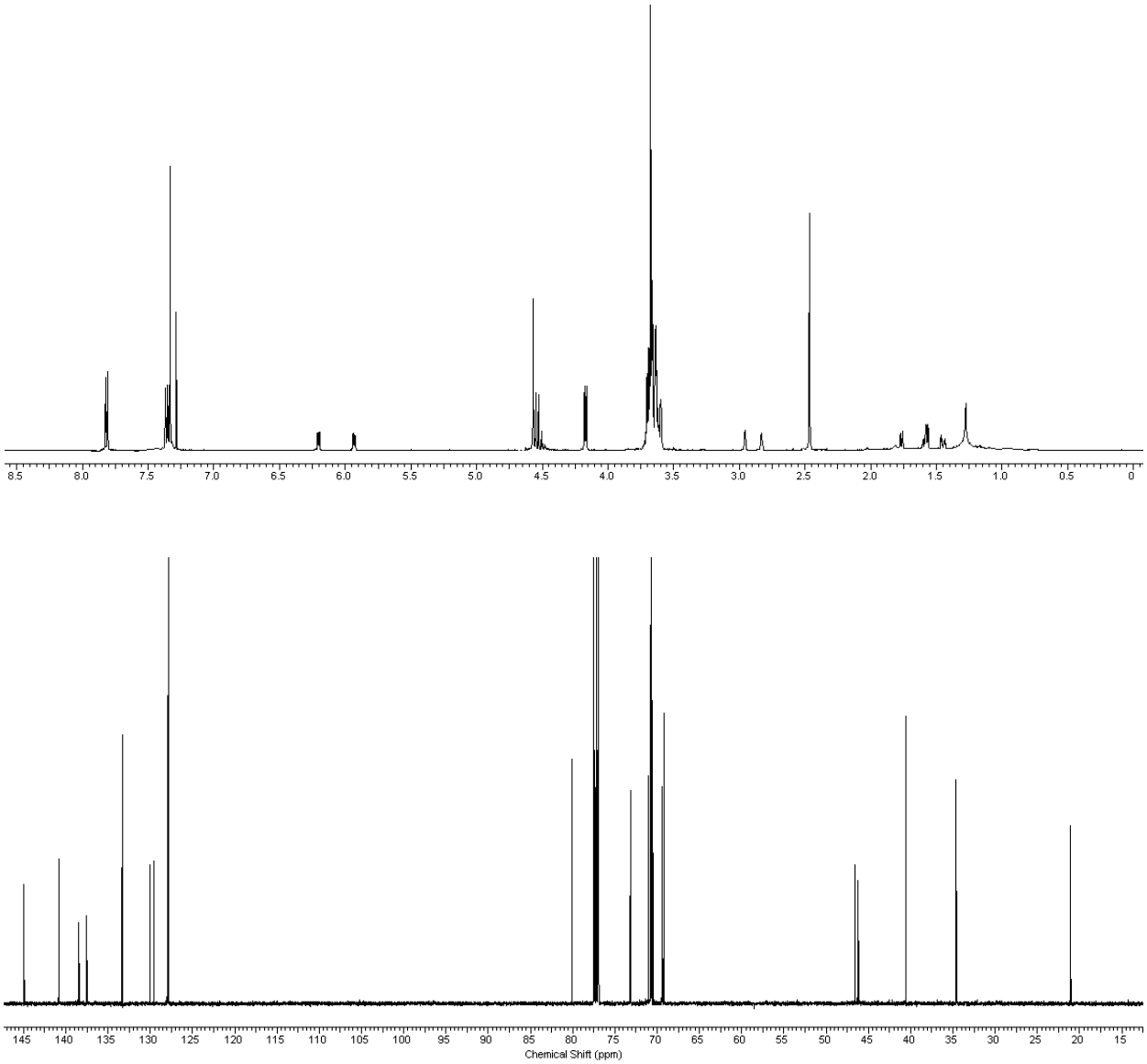

Fig. S1. The ^{1}H (top) and ^{13}C NMR (bottom) spectra for 1-[4-({bicyclo[2.2.1]hept-5-en-2-yloxy}methyl)phenyl]-2,5,8,11,14,17-hexaoxanonadecan-19-yl 4 ethylbenzene-1-sulfonate (**4**).

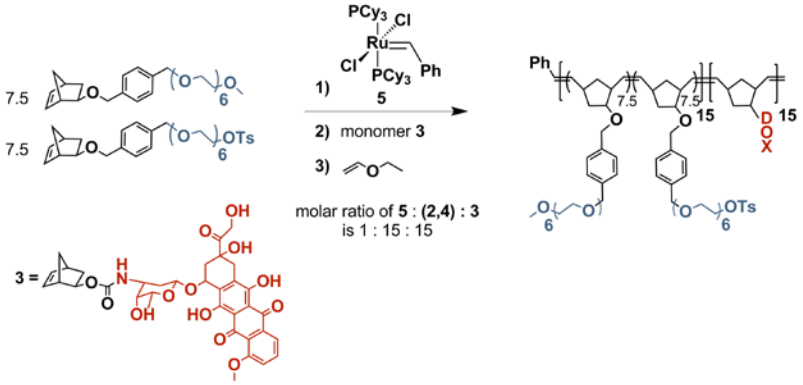

Synthesis of block copolymer (2-*co*-4)$_{15}$-*b*-3$_{15}$. In an inert-atmosphere glovebox, monomers **2** (11.8 mg, 0.0231 mmol) and **4** (15 mg, 0.0231 mmol) were dissolved in an anhydrous mixture of $CHCl_3$:MeOH (9:1 v/v, 2 mL) in a 20-mL scintillation vial equipped with a magnetic stirring bar. A stock solution of catalyst **5** (5 mg) in CH_2Cl_2 (5 mL) was prepared, a portion of which (2.54 mL, 3.08 μmol) was added to the vial containing the mixture of monomers **2** and **4** under vigorous stirring. The resulting reaction mixture was stirred at room temperature for 30 min, at which time an aliquot (100 μL) was removed and quenched with excess ethyl vinyl ether. A portion of this quenched aliquot was evaporated to dryness, redissolved in $CDCl_3$, and analyzed by ^{1}H NMR spectroscopy, which indicated complete consumption of the monomer. The remaining portion was evaporated to dryness, dissolved in HPLC-grade THF, and subjected to GPC analysis (M_n = 10000 (theoretical M_n = 9000), PDI = 1.11).

Immediately after aliquot removal, a solution of monomer **3** (30.4 mg, 0.0447 mmol) in a mixture of $CHCl_3$:MeOH (9:1 v/v, 1.5 mL) was added to the reaction vial and the resulting polymerization mixture was stirred for an additional 45 min before being terminated with the addition of ethyl vinyl ether (1 mL). The reaction mixture was added quickly into vigorously stirred cold (-10 °C) pentanes (200 mL), and the resulting precipitate was isolated *via* vacuum filtration and washed thoroughly with fresh pentanes to afford the product copolymer quantitatively as a dark red solid (GPC: M_n = 19000 (theoretical M_n = 19000), PDI = 1.13). ^{1}H NMR ($CDCl_3$, Fig. S2): δ 1.08 (bs), 1.25 (bd), 1.41 (bs), 1.81 (bs), 2.18 (bs), 2.36 (bs), 2.53 (bd), 2.86-3.22 (bm), 3.35-3.94 (bm), 4.11 (bs), 4.14 (bs), 4.37-4.64 (bm), 5.12-5.56 (bm), 7.22-7.61 (bm), 7.79 (bd), 7.96 (bd).

A series of block copolymers were synthesized with varying stoichiometric ratios of monomers **2**:**4** (7:3, 1:1, 3:7, 0:1) in the hydrophilic block of copolymer (**2**-*co*-**4**)$_{15}$-*b*-**3**$_{15}$. Unfortunately, the copolymers with 3:7 and 0:1 ratios of **2**:**4** did not polymerize to completion. To maximize the chemical handles that can subsequently be used for surface functionalization of the PNPs, we employed the block copolymer with the equimolar ratio of the hydrophilic monomers.

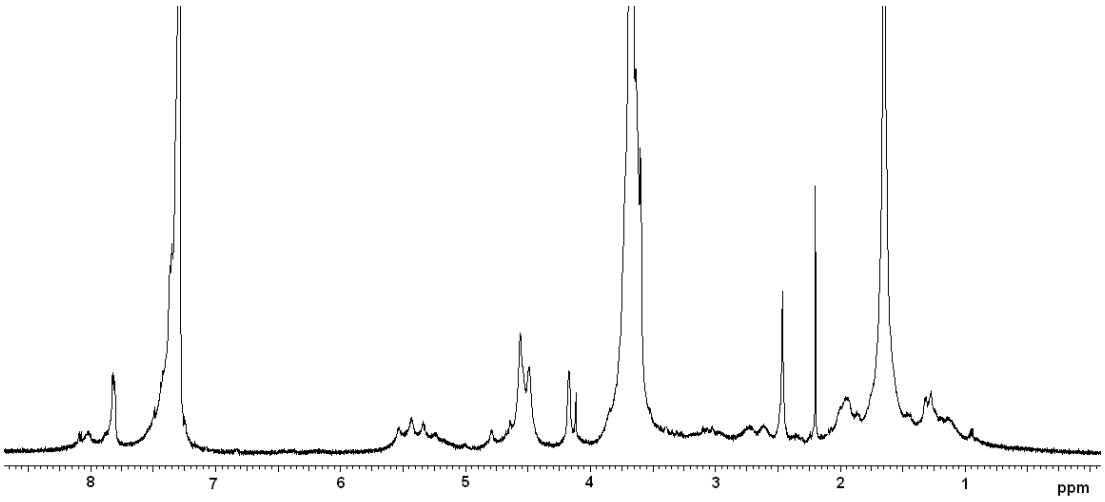

Fig. S2. The ^{1}H NMR spectrum of block copolymer (**2**-*co*-**4**)$_{15}$-*b*-**3**$_{15}$.

Attempted synthesis of block copolymer (3$_{15}$-*b*-(2-*co*-4)$_{15}$). In an inert-atmosphere glovebox, monomer **3** (5 mg, 7.35 µmol) was dissolved in an anhydrous mixture of $CHCl_3$:MeOH (9:1 v/v, 1 mL) in a 20-mL scintillation vial equipped with a magnetic stirring bar. A stock solution of catalyst **5** (5 mg) in CH_2Cl_2 (5 mL) was prepared, a portion of which (0.4 mL, 0.49 µmol) was added to the vial containing monomer **3** under vigorous stirring. The resulting reaction mixture was stirred at room temperature for 1 h, at which time an aliquot (100 µL) was removed and quenched with excess ethyl vinyl ether. A portion of this quenched aliquot was evaporated to dryness, redissolved in $CDCl_3$, and analyzed by ^{1}H NMR spectroscopy, which indicated incomplete consumption of the monomer **3** (Fig. S3). The remaining portion was evaporated to dryness, dissolved in HPLC-grade THF, and subjected to GPC analysis (M_n = 3600 (theoretical M_n = 11000), PDI = 1.29). Due to the lack of complete polymerization of monomer **3**, we did not attempt to copolymerize the hydrophilic monomers **2** and **4** subsequently.

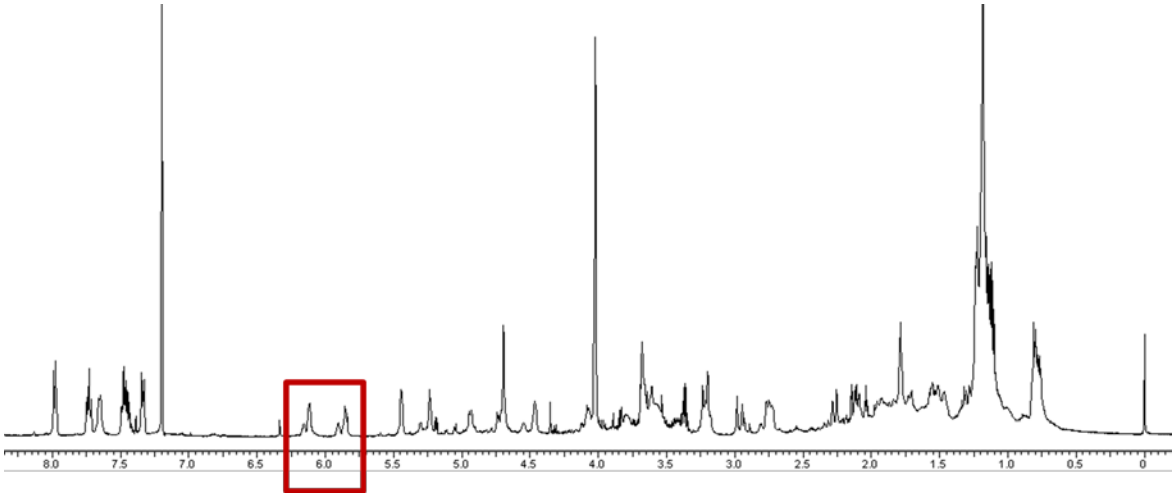

Fig. S3. The ^{1}H NMR spectrum of the reaction mixture after an attempted synthesis of block copolymer (**3**$_{15}$-*b*-(**2**-*co*-**4**)$_{15}$. The polymerization of monomer **3** by catalyst **5** clearly shows left-over norbornene monomer peaks (red box), indicating incomplete polymerization.

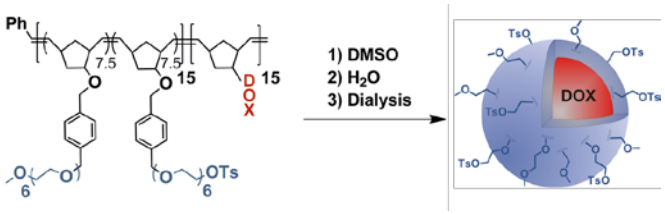

Suspension of tosyl-functionalized doxorubicin-containing PNPs in phosphate-buffered saline (PBS). An aliquot of the PNPs (500 µL) derived from copolymer (**2**-*co*-**4**)$_{15}$-*b*-**3**$_{15}$ was transferred to a 1.5-mL safe-lock Eppendorf tube and centrifuged for 30 min at 10K rpm to a solid pellet. The supernatant was removed and the PNPs were re-suspended in PBS (500 µL, 10 mM, pH 7.4, 150 mM [NaCl]). Unfortunately, characterization of the PNP suspension in PBS revealed a loss of the original well-defined morphology of the parent PNPs as observed by TEM (Fig. S4e) and DLS (Fig. S4g: D_H = 895 ± 98 nm, PDI = 0.204). Attempts to reverse PNP aggregation through a dialytic removal of salts were unsuccessful as observed by TEM (Fig. S4i) and DLS (Fig. S4k: D_H = 833 ± 79 nm, PDI = 0.379).

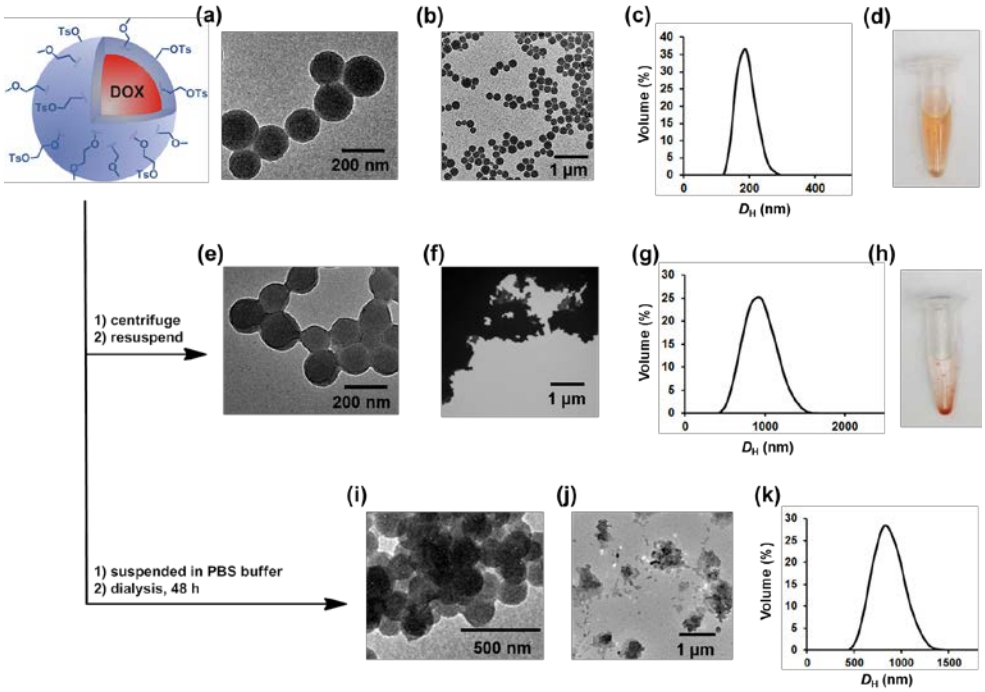

Fig. S4. Left: A schematic representation of the PNPs derived from block copolymer (**2**-*co*-**4**)$_{15}$-*b*-**3**$_{15}$. Right top panels: (a) a representative TEM image of these PNPs in ultrapure deionized water; (b) a low-magnification TEM image of this material; (c) the corresponding D_H distribution of these PNPs as measured by DLS; and (d) a photograph of an aliquot of the PNPs in an Eppendorf tube. Right center panels: (e) a representative TEM image of these PNPs upon centrifugation and resuspension in PBS (10 mM, pH 7.4, 150 mM [NaCl]); (f) a low-magnification TEM image of this material; (g) the corresponding D_H distribution of these PNPs; and (h) a photograph of an aliquot of the PNPs in an Eppendorf tube, clearly indicating PNP aggregation. Right bottom panels: (i) a representative TEM image of the PNPs suspended in PBS and immediately dialyzed against ultrapure deionized water over a 48 h period; (j) a low-magnification TEM image of this material; and (k) the corresponding D_H distribution of these PNPs after the dialysis indicating the irreversibility of the PNP aggregation.

IV. Attempted steric modification *via* pre- and post-nanoparticle-formation methods.

The pre-nanoparticle-formation incorporation of Poloxamer 188 into PNPs derived from block copolymers $\mathbf{2}_{15}$-*b*-$\mathbf{3}_{15}$ and (2**-*co*-**4**)$_{15}$-*b*-$\mathbf{3}_{15}$.**

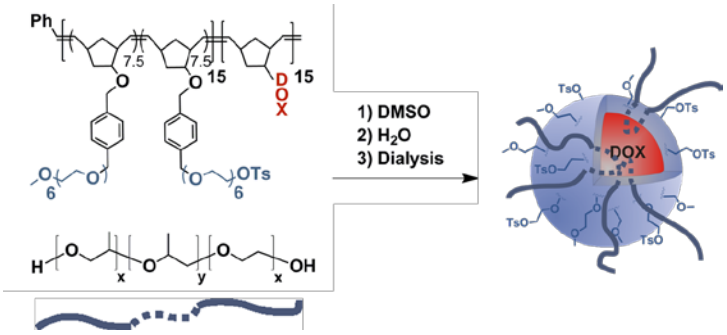

Poloxamer 188 incorporation in the PNP matrix. An aliquot (2.5 mL) of a stock solution of the block copolymer $\mathbf{2}_{15}$-*b*-$\mathbf{3}_{15}$ or (**2**-*co*-**4**)$_{15}$-*b*-$\mathbf{3}_{15}$ (0.01 wt%) in DMSO was transferred to a 4-mL scintillation vial and set to stir vigorously. Poloxamer 188 (MW = 8350 g/mol, 1.1 mg (100 wt%)) was added to this stirring copolymer solution followed by the addition of ultrapure deionized water at a rate of 1 drop (10 µL, 0.35 wt%) every 10 s using a 2-20 µL micro-pipette until the mixture contained 18 wt% water. The resulting cloudy mixture was placed in a 3-mL dialysis cassette and dialyzed against ultrapure deionized water (500 mL), with the dialate changed every 2 h. Complete absence of DMSO in the dialate after 48 h was verified by UV-vis spectroscopy as indicated by the disappearance of the UV cut-off for DMSO at 268 nm. To confirm the incorporation of Poloxamer 188 within the PNP matrix, a larger batch of these PNPs were prepared, evaporated to dryness, dissolved in HPLC-grade THF, and subjected to GPC analysis: copolymer $\mathbf{2}_{15}$-*b*-$\mathbf{3}_{15}$ M_n = 19000 (theoretical M_n = 18000), PDI = 1.05; Poloxamer 188 M_n = 9000 (theoretical M_n = 8000), PDI = 1.18) (Fig. S5a); copolymer (**2**-*co*-**4**)$_{15}$-*b*-$\mathbf{3}_{15}$ M_n = 20000 (theoretical M_n = 19000), PDI = 1.07; Poloxamer 188 M_n = 10000 (theoretical M_n = 8000), PDI = 1.23) (Fig. S5b).

DLS analysis of the final Poloxamer 188-incorported PNP aqueous suspension derived from copolymers $\mathbf{2}_{15}$-*b*-$\mathbf{3}_{15}$ and (**2**-*co*-**4**)$_{15}$-*b*-$\mathbf{3}_{15}$ revealed narrowly dispersed PNPs with average diameters (D_H) of 188 ± 16 nm and 194 ± 15 nm and corresponding polydispersity indices (PDI) of 0.015 and 0.023, respectively (Fig. S6c and S6h). TEM analysis indicated a uniform size distribution for the PNPs in the solid state, with an average diameter of ~200 nm (Fig. S6a and S6f) that is consistent with the DLS data. An aliquot of the PNPs (500 µL) was transferred to a 1.5-mL safe-lock Eppendorf tube and centrifuged for 30 min at 10K rpm to a solid pellet. The supernatant was removed and the PNPs were re-suspended in PBS (500 µL, 10 mM, pH = 7.4, [NaCl] = 150 mM). Unfortunately, characterization of the PNP suspension in PBS revealed a loss of the original well-defined morphology of the parent PNPs as observed by TEM (Fig. S6d and S6i) and DLS (for copolymer $\mathbf{2}_{15}$-*b*-$\mathbf{3}_{15}$ Fig. S6e: D_H = 642 ± 39 nm, PDI = 0.711; for copolymer (**2**-*co*-**4**)$_{15}$-*b*-$\mathbf{3}_{15}$: Fig. S6j: D_H = 666 ± 63 nm, PDI = 0.583).

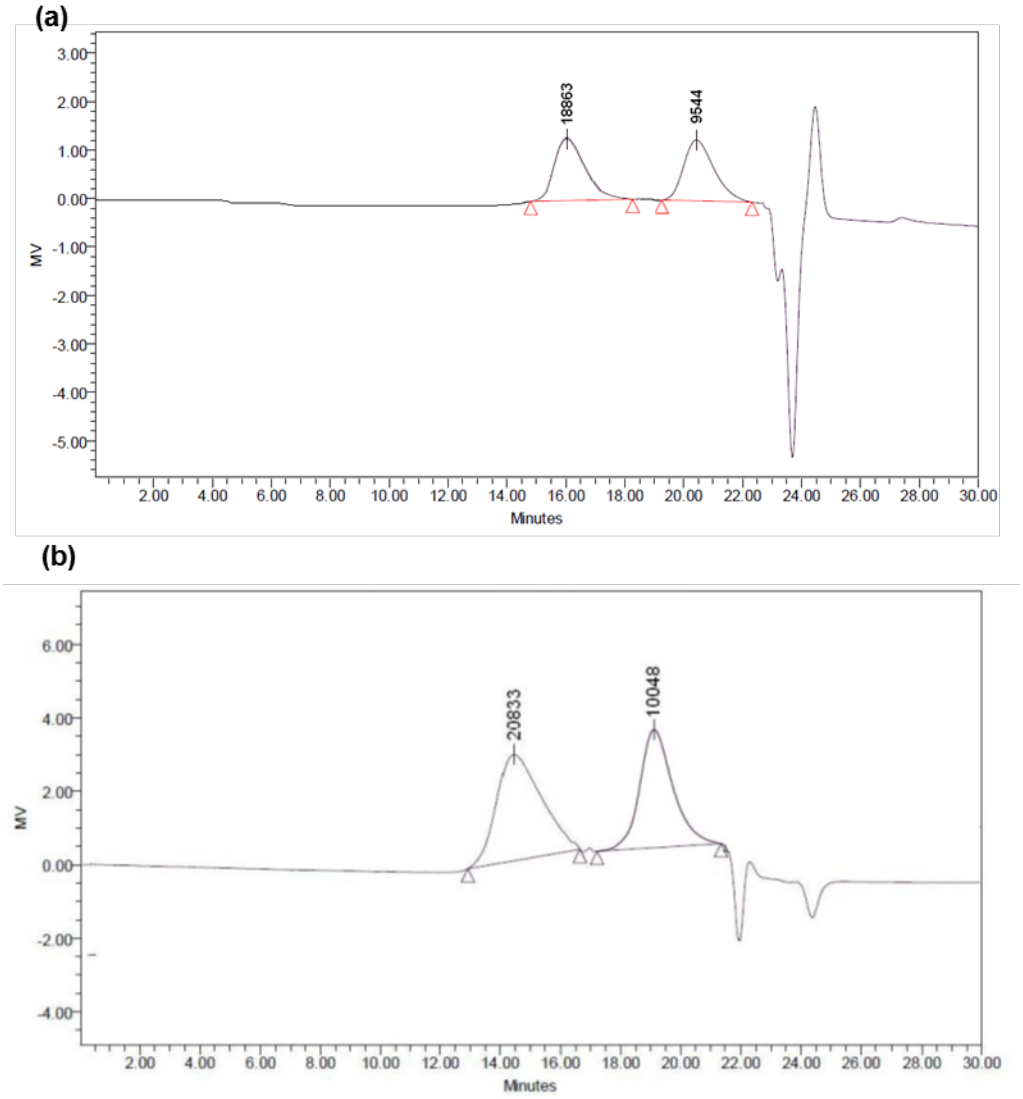

Fig. S5. Analytical GPC traces of the 100 wt% Poloxamer 188-incorporated PNPs derived from block copolymers $\mathbf{2}_{15}$-*b*-$\mathbf{3}_{15}$ (a) and (**2**-*co*-**4**)$_{15}$-*b*-$\mathbf{3}_{15}$ (b), indicating complete integration of Poloxamer 188 into the PNP matrix.

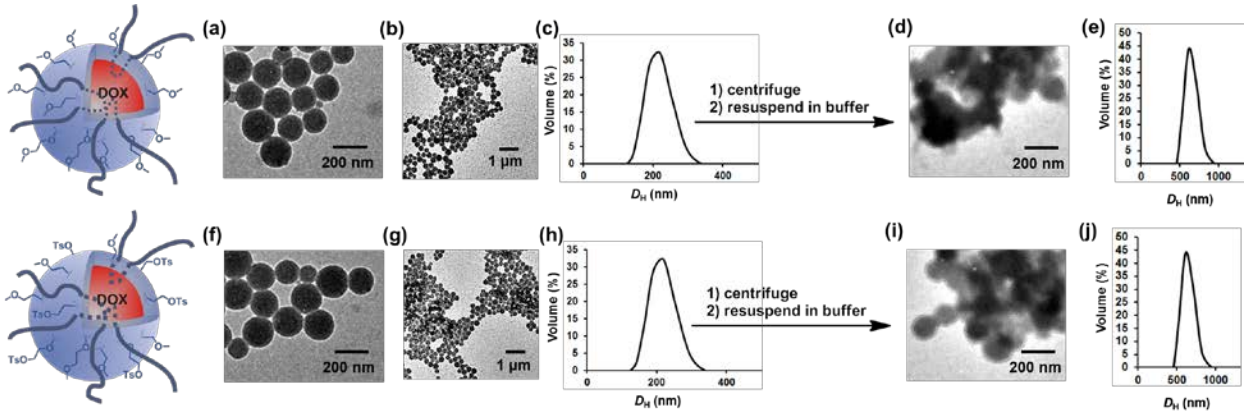

Fig. S6. A schematic representation of the Poloxamer 188-incorporated PNPs derived from block copolymers

$\mathbf{2}_{15}$-*b*-$\mathbf{3}_{15}$ (top) and (**2**-*co*-**4**)$_{15}$-*b*-$\mathbf{3}_{15}$ (bottom). Left: (a and f) representative TEM images of these PNPs in ultrapure deionized water; (b and g) low-magnification TEM images of these materials; and (c and h) the corresponding D_H distributions of these PNPs as measured by DLS. Right: (d and i) representative TEM images of these PNPs upon centrifugation and resuspension in PBS (10 mM, pH 7.4, 150 mM [NaCl]) and (e and j) the corresponding D_H distributions of these PNPs, clearly indicating loss of the original narrowly dispersed suspension.

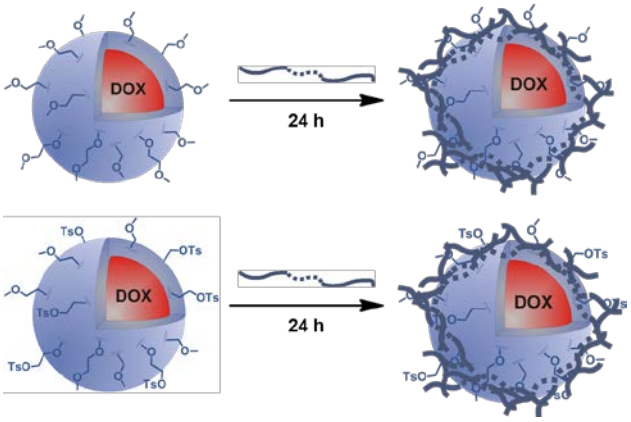

The post-nanoparticle-formation incorporation of Poloxamer 188 on the PNP surface as a stabilizer. In a 1.5 mL safe-lock Eppendorf tube, an aqueous solution of Poloxamer 188 (25 mg/500 µL) was added to an aliquot (1 mL) of the aqueous PNP suspension derived from copolymers $\mathbf{2}_{15}$-*b*-$\mathbf{3}_{15}$ or (**2**-*co*-**4**)$_{15}$-*b*-$\mathbf{3}_{15}$. The resulting mixture was allowed to incubate on a platform shaker (1150 rpm) for 24 h at room temperature , followed by centrifugation for 30 min at 10K rpm to a solid pellet. The supernatant was removed and the PNPs were re-suspended in ultrapure deionized water. DLS analysis of the final PNP aqueous suspension derived from copolymers $\mathbf{2}_{15}$-*b*-$\mathbf{3}_{15}$ and (**2**-*co*-**4**)$_{15}$-*b*-$\mathbf{3}_{15}$ revealed narrowly dispersed PNPs with average diameters (D_H) of 178 ± 19 nm and 181 ± 16 nm and corresponding polydispersity indices (PDI) of 0.078 and 0.066, respectively (Fig. S7c and S7h). TEM analysis indicated a uniform size distribution for the PNPs in the solid state, with an average diameter of ~200 nm (Fig. S7a and S7f) that is consistent with the DLS data. Unfortunately, resuspension of these Poloxamer-coated PNPs derived from block copolymers $\mathbf{2}_{15}$-*b*-$\mathbf{3}_{15}$ and (**2**-*co*-**4**)$_{15}$-*b*-$\mathbf{3}_{15}$ in PBS (1 mL, 10 mM, pH = 8.5, [NaCl] = 150 mM) resulted in the loss of the original well-defined spherical morphology of the parent PNPs, as observed by TEM (Fig. S7d and S7i) and DLS (for copolymer $\mathbf{2}_{15}$-*b*-$\mathbf{3}_{15}$, Fig. S7e: D_H = 432 ± 27 nm, PDI = 0.717; for copolymer (**2**-*co*-**4**)$_{15}$-*b*-$\mathbf{3}_{15}$, Fig. S7j: D_H = 581 ± 54 nm, PDI = 0.424). PNPs derived from both copolymers were incubated for varing times (0, 6, 12, 24, 36, 48, and 72 h) with Poloxamer 188 under the aforementioned conditions to determine if increasing the incubation period would help stabilize the PNPs. Unfortunately, DLS analysis revealed that these PNP suspensions continued to aggregate in PBS (Fig. S8).

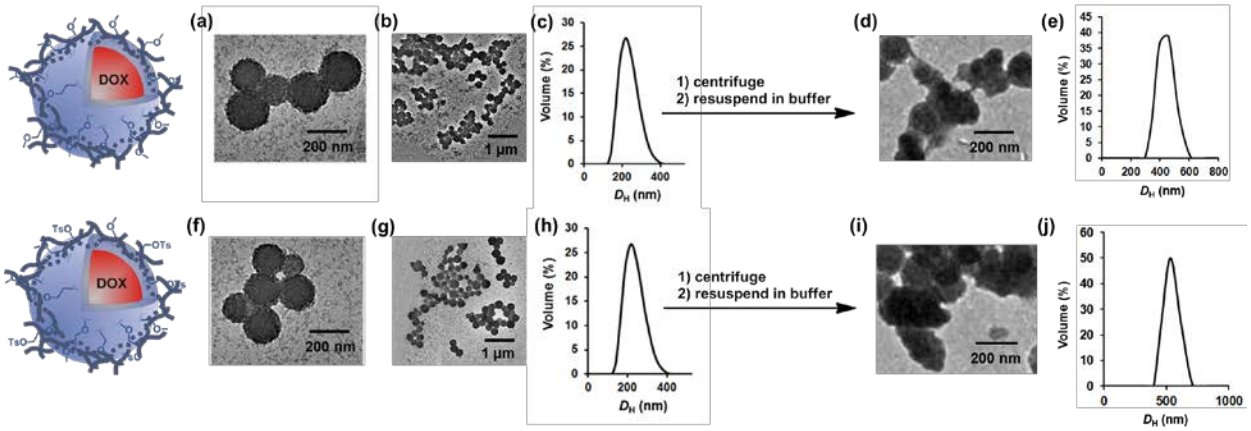

Fig. S7. A schematic representation of the Poloxamer 188-coated PNPs derived from block copolymers $\mathbf{2}_{15}$-*b*-$\mathbf{3}_{15}$ (top) and (**2**-*co*-**4**)$_{15}$-*b*-$\mathbf{3}_{15}$ (bottom). Left: (a and f) representative TEM images of these PNPs in ultrapure deionized water; (b and g) low-magnification TEM images of these materials; and (c and h) the corresponding D_H distributions of these PNPs as measured by DLS. Right: (d and i) representative TEM images of these PNPs upon centrifugation and resuspension in PBS (10 mM, pH 7.4, 150 mM [NaCl]) and (e and j) the corresponding D_H distributions of these PNPs, clearly indicating loss of the original narrowly dispersed suspension.

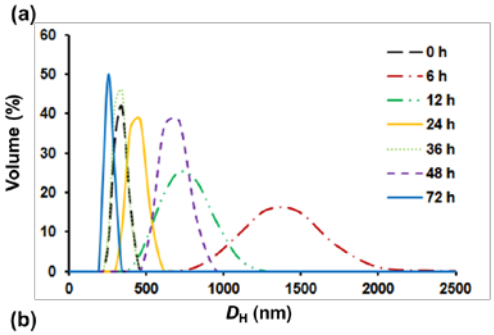

Time	Size (PDI)
0 h	328 ± 20 nm (0.831)
6 h	1344 ± 130 nm (0.203)
12 h	726 ± 77 nm (0.216)
24 h	432 ± 27 nm (0.717)
36 h	348 ± 25 nm (0.466)
48 h	670 ± 42 nm (0.781)
72 h	256 ± 13 nm (1.000)

Time	Size (PDI)
0 h	941 ± 55 nm (0.636)
6 h	961 ± 50 nm (0.802)
12 h	225 ± 22 nm (0.177)
24 h	581 ± 54 nm (0.424)
36 h	1239 ± 75 nm (0.589)
48 h	833 ± 65 nm (0.590)
72 h	300 ± 37 nm (0.281)

Fig. S8. DLS data of the Poloxamer 188-coated PNPs derived from block copolymers (a) $\mathbf{2}_{15}$-*b*-$\mathbf{3}_{15}$ and (b) (**2**-*co*-**4**)$_{15}$-*b*-$\mathbf{3}_{15}$ suspended in PBS showing an aggregation behavior that widely fluctuates over a 72 h period.

Synthesis of monomer 7 and block copolymer (2-*co*-7)$_{15}$-*b*-3$_{15}$.

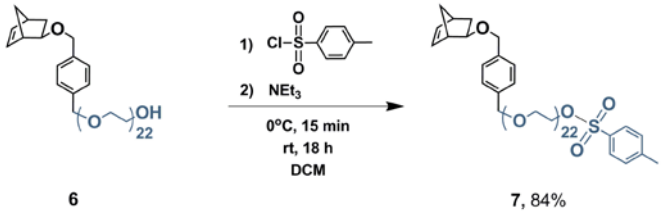

6 7, 84%

1-(4-((Bicyclo[2.2.1]hept-5-en-2-yloxy)methyl)phenyl)-2,5,8,11,14,17,20,23,26,29,32,35,38,41,44,47,50,53,56,59, 62,65-docosaoxaheptahexacontan-67-yl 4-methylbenzenesulfonate (7). Monomer **6** (783 mg, 76% yield) was synthesized following the previously described (see synthesis of monomer **4** above) modification of a published procedure[S2] and employing PEG 1000 instead of hexa(ethylene glycol). Using a similar protocol as that specified for the synthesis of **4**, monomer **7** was synthesized and isolated as a dark-yellow oil (71 mg, 84% yield). ^{1}H NMR ($CDCl_3$, Fig. S9): δ 1.35-1.71 (m, 4H, 3- and 7-norbornenyl-H_2), 2.45 (s, 3H, aromatic-CH_3), 2.82 (b, 1H, 1-norbornenyl-*H*), 2.94 (b, 1H, 4-norbornenyl-*H*), 3.59-3.70 (m, 86H, OCH_2CH_2O), 4.16 (t, 2H, CH_2CH_2OSO$_2$), 4.45-4.56 (m, 5H, CH_2-C_6H_4-CH_2 and 2-norbornenyl-*H*), 5.92 (m, 1H, 6-norbornenyl-*H*), 6.23 (m, 1H, 5-norbornenyl-*H*), 7.32 (b, 4H, aromatic-*H*), 7.35 (d, 2H, aromatic-*H*), 7.81 (d, 2H, aromatic-*H*). ESIMS (positive mode): *m/z* calculated for $C_{66}H_{48}O_{25}S$ $[M + Na]^+$: 1353.66. Found: 1353.89.

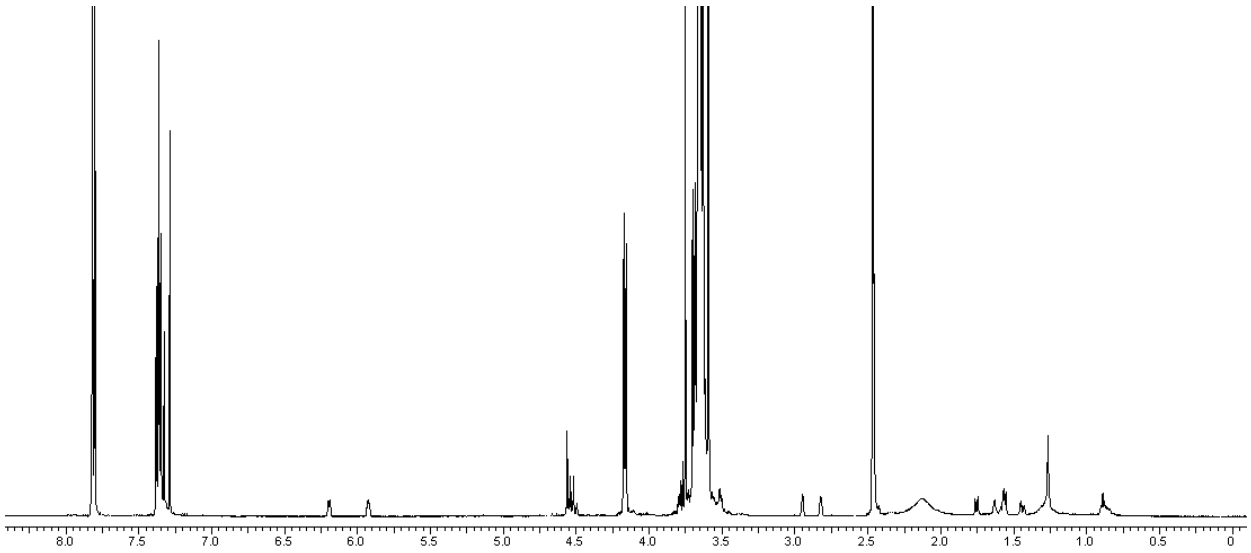

Fig. S9. The ^{1}H NMR spectrum for 1-(4-((bicyclo[2.2.1]hept-5-en-2-yloxy)methyl)phenyl)-2,5,8,11,14,17,20,23,26,29,32,35,38,41,44,47,50,53,56,59, 62,65-docosaoxaheptahexacontan-67-yl 4-methylbenzenesulfonate (**7**).

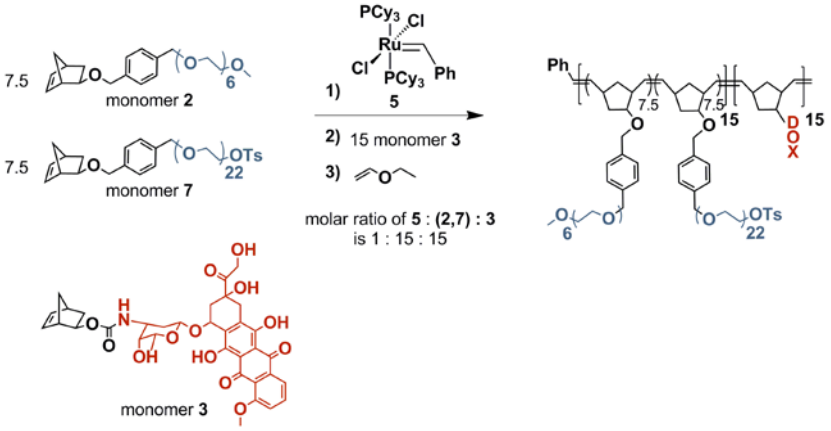

Synthesis of block copolymer (2-*co*-7)$_{15}$-*b*-3$_{15}$. Using a protocol similar to that reported above for the synthesis of (**2**-*co*-**4**)$_{15}$-*b*-**3**$_{15}$, block copolymer (**2**-*co*-**7**)$_{15}$-*b*-**3**$_{15}$ was synthesized and isolated quantitatively. ^{1}H NMR ($CDCl_3$, Fig. S10): δ 1.08 (bs), 1.25 (bd), 1.41 (bs), 1.81 (bs), 2.18 (bs), 2.36 (bs), 2.53 (bd), 2.86-3.22 (bm), 3.35-3.94 (bm), 4.11 (bs), 4.14 (bs), 4.37-4.64 (bm), 5.12-5.56 (bm), 7.22-7.61 (bm), 7.79 (bd), 7.96 (bd). GPC: M_n = 25000 (theoretical M_n = 24000), PDI = 1.09. GPC for the first block: M_n = 14000 (theoretical M_n = 14000), PDI = 1.17.

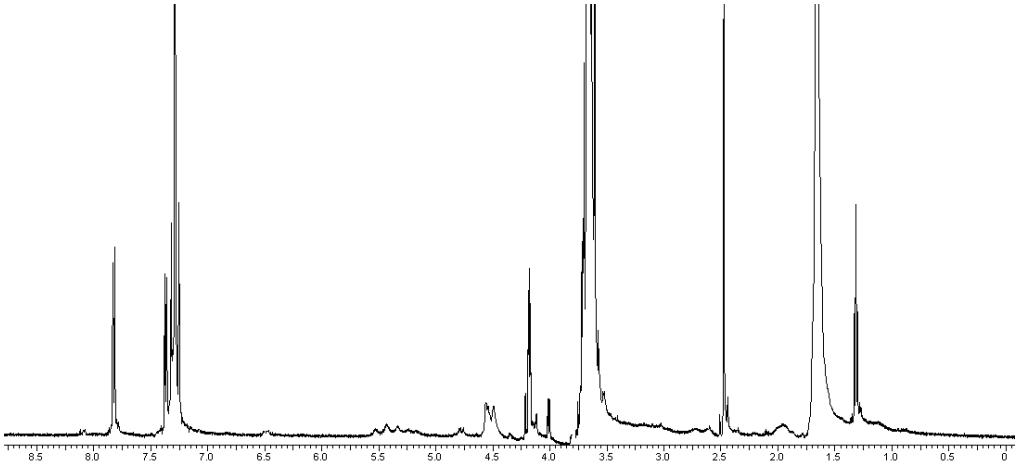

Fig. S10. The ^{1}H NMR spectrum of block copolymer (**2**-*co*-**7**)$_{15}$-*b*-**3**$_{15}$.

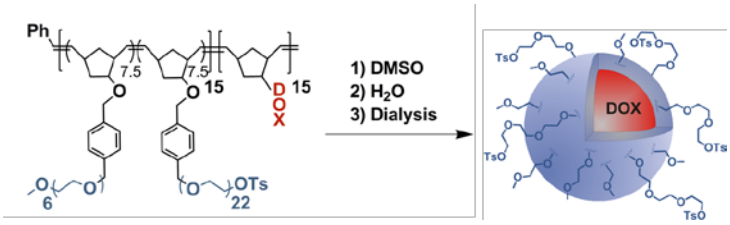

PNP preparation from block copolymer (2-*co*-7)$_{15}$-*b*-3$_{15}$. Using a similar protocol as described in the Materials and methods section, "General procedure for the preparation of nanoparticle dispersions" subsection, in the main manuscript, aqueous polymer nanoparticle dispersions of the block copolymer (**2**-*co*-**7**)$_{15}$-*b*-**3**$_{15}$ (0.01 wt%) were prepared. DLS analysis of the final PNP aqueous dispersion revealed narrowly dispersed PNPs with an average diameter (D_H) of 159 ± 16 nm and a corresponding PDI of 0.033 (Fig. S11c). TEM analysis indicated a uniform size distribution for the PNPs in the solid state, with an average diameter of ~150 nm (Fig. S11a) that is consistent with the DLS data. An aliquot of the PNPs (500 µL) was transferred to a 1.5-mL safe-lock Eppendorf tube and centrifuged for 30 min at 10K rpm to a solid pellet. The supernatant was removed and the PNPs were re-suspended

in PBS (500 µL, 10 mM, pH = 7.4, [NaCl] = 150 mM). Unfortunately, characterization of the PNP suspension in PBS revealed a loss of the original well-defined spherical morphology of the parent PNPs, as observed by TEM and DLS (Fig. S11d and S11f: D_H = 769 ± 49 nm, PDI = 0.434).

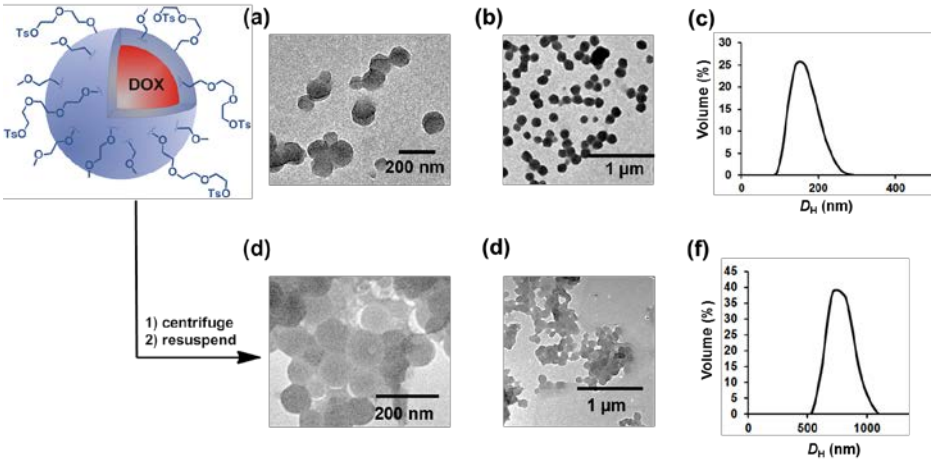

Fig. S11. Left: A schematic representation of the PNPs derived from block copolymer (**2**-*co*-**7**)$_{15}$-*b*-**3**$_{15}$. Right top panels: (a) a representative TEM image of these PNPs in ultrapure deionized water; (b) a low-magnification TEM image of this material; and (c) the corresponding D_H distribution of these PNPs as measured by DLS. Right bottom panels: (d) a representative TEM image of these PNPs upon centrifugation and resuspension in PBS (10 mM, pH 7.4, 150 mM [NaCl]); (e) a low-magnification TEM image of this material; and (f) the corresponding D_H distribution of these PNPs, clearly indicating loss of the original narrowly dispersed suspension.

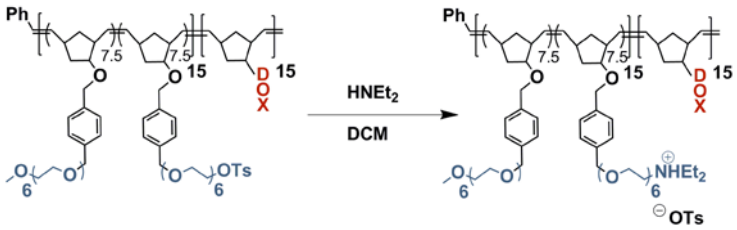

Displacement of tosylate groups on copolymer (2-*co*-4)$_{15}$-*b*-3$_{15}$. Copolymer (**2**-*co*-**4**)$_{15}$-*b*-**3**$_{15}$ (25 mg, 1.32 µmol) was dissolved in dry DCM (5 mL) in a 50-mL Schlenk flask. After the addition of diethylamine (0.5 mL, 4.82 mmol) using a gas-tight syringe, the reaction mixture was allowed to stir overnight at room temperature. The reaction mixture was then added quickly into vigorously stirred cold (-10 °C) pentanes (200 mL), and the resulting precipitate was isolated *via* vacuum filtration and washed thoroughly with fresh pentanes to afford the product copolymer, in 70% of the original mass, as a dark red solid. ^{1}H NMR ($CDCl_3$, Fig. S12): δ 1.10 (bs), 1.23 (bd), 1.38 (bs), 1.84 (bs), 2.35 (bs), 2.40 (bs), 2.55 (bd), 2.91-3.09 (bm), 3.55-3.78 (bm), 4.09 (bs), 4.17 (bs), 4.41-4.58 (bm), 5.10-5.55 (bm), 7.24-7.41 (bm), 7.83 (bd), 9.50 (bs).

Using a similar protocol as described in the Materials and methods section, "General procedure for the preparation of nanoparticle dispersions" subsection, in the main manuscript, aqueous polymer nanoparticle dispersions of the amine-modified copolymer derived from copolymer (**2**-*co*-**4**)$_{15}$-*b*-**3**$_{15}$ (0.01 wt%) were prepared. Unfortunately, TEM analysis indicated that the PNPs had a polydisperse size distribution in the solid state (Fig. S13a), consistent with the DLS data (Fig. S13c: D_H = 662 ± 59 nm, PDI = 0.216).

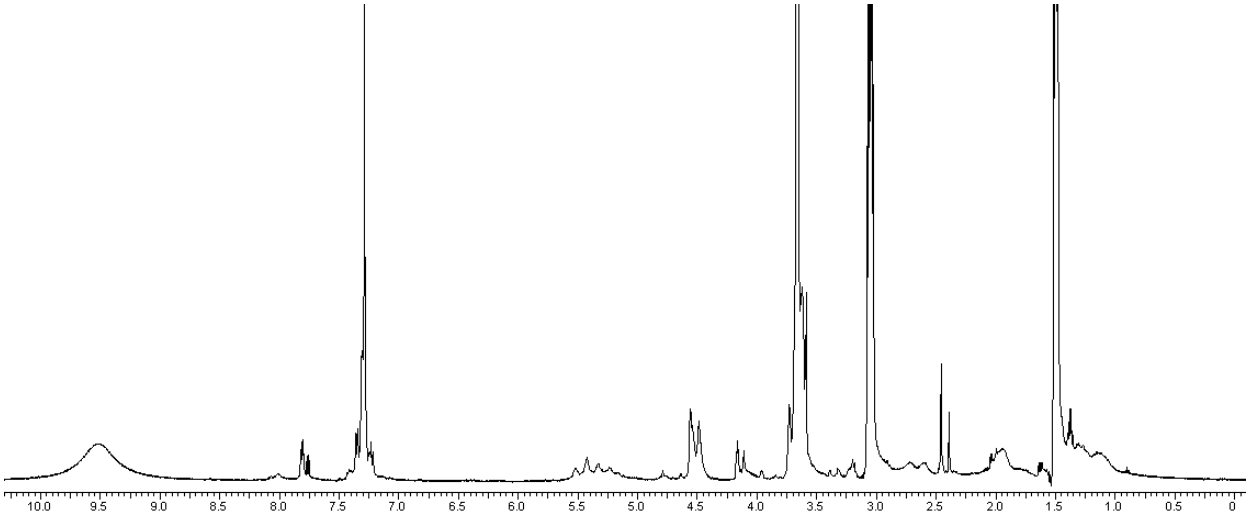

Fig. S12. The ^{1}H NMR spectrum of the diethylamine-modified block copolymer (**2**-*co*-**4**)$_{15}$-*b*-**3**$_{15}$.

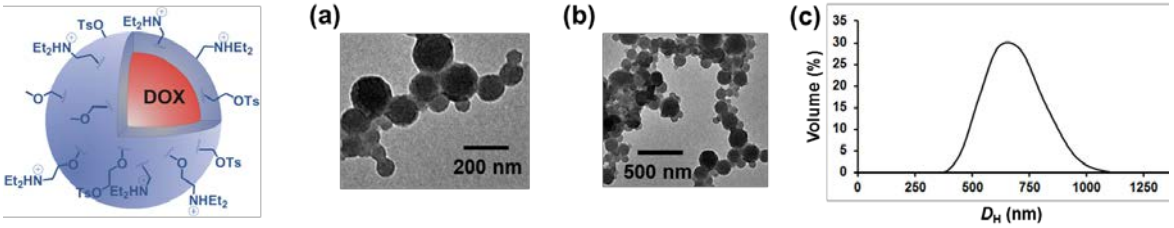

Fig. S13. Left: A schematic representation of the PNPs derived from diethylamine-modified block copolymer (**2**-*co*-**4**)$_{15}$-*b*-**3**$_{15}$. Right: (a) a representative TEM image of these PNPs in ultrapure deionized water; (b) a low-magnification TEM image of this material; and (c) the corresponding D_H distribution of these PNPs as measured by DLS, clearly indicating a polydisperse sample.

V. Surface functionalization of PNPs derived from block copolymer (2-*co*-4)$_{15}$-*b*-3$_{15}$.

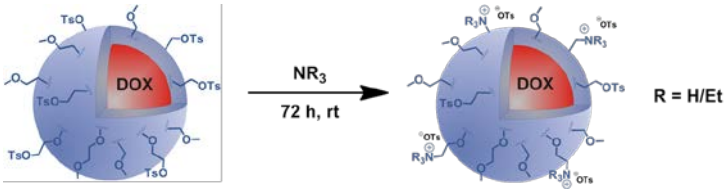

Characterization of NEt$_3$-modified PNPs and assessment of PNP dispersibility as a function of time. NEt$_3$-modified PNPs retained the narrow size disribution of the parent PNPs (PDI = 0.053 with D_H = 190 ± 18 nm), as indicated by DLS and TEM (Fig. S14). To further probe the dispersibility of PNPs over time, the PNP surface displacement reaction was monitored at 0, 6, 12, 24, 36, 48, and 72 h (Fig. S14e). Improved PNP dispersibility in PBS was observed after a period of 12 h, indicating that sufficient surface tosylate groups were displaced by NEt$_3$ to result in charge stabilization of the PNPs.

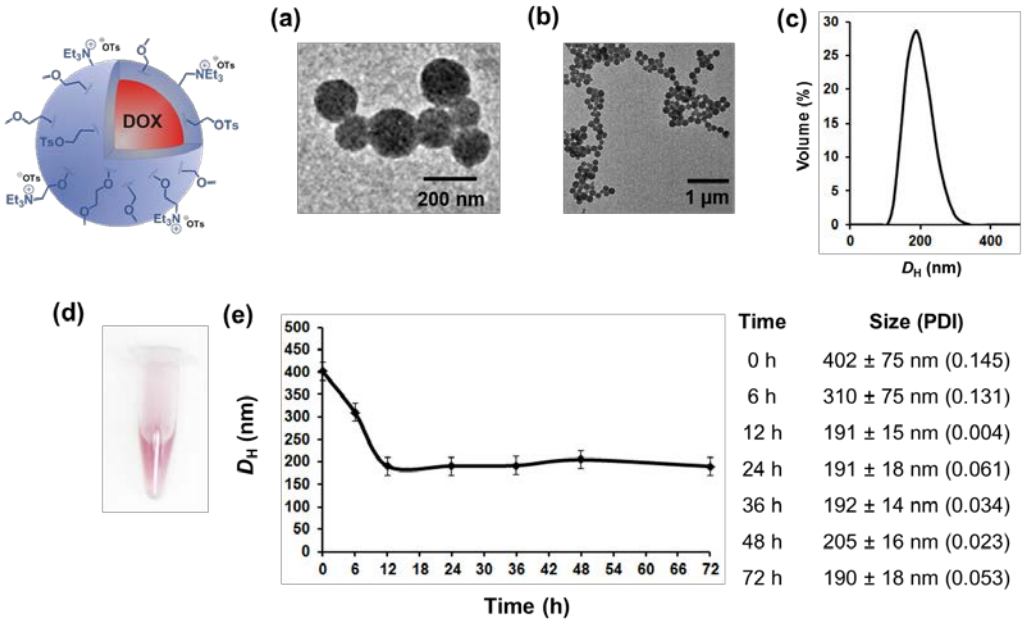

Fig. S14. A schematic representation of the NEt_3-modified PNPs derived from copolymer (**2**-*co*-**4**)$_{15}$-*b*-**3**$_{15}$. (a) A representative TEM image of this material after being suspended in PBS (10 mM, pH 7.4, 150 mM [NaCl]), indicating a well-defined, narrowly dispersed spherical morphology; (b) a low-magnification TEM image of this material; (c) D_H distribution of these PNPs in PBS as measured by DLS; (d) a photograph of an aliquot of the PNPs re-suspended in PBS in an Eppendorf tube, clearly indicating retention of PNP dispersibility upon surface modification; and (e) DLS data showing the stabilization of NEt_3-modified PNPs as a function of a time. PNPs are stabilized in PBS after a 12 h incubation period with NEt_3.

Characterization of $HNEt_2$-modified PNPs and assessment of PNP dispersibility as a function of time. $HNEt_2$-modified PNPs retained the narrow size disribution of the parent PNPs (PDI = 0.053 with D_H = 190 ± 18 nm), as indicated by DLS and TEM (Fig. S15). To further probe the stabilization behavior over time, the PNP surface displacement reaction was monitored at 0, 6, 12, 24, 36, 48, and 72 h (Fig. S15e). Improved PNP dispersibility in PBS was observed after a period of 12 h, indicating that sufficient surface tosylate groups were displaced by $HNEt_2$ to result in charge stabilization of the PNPs.

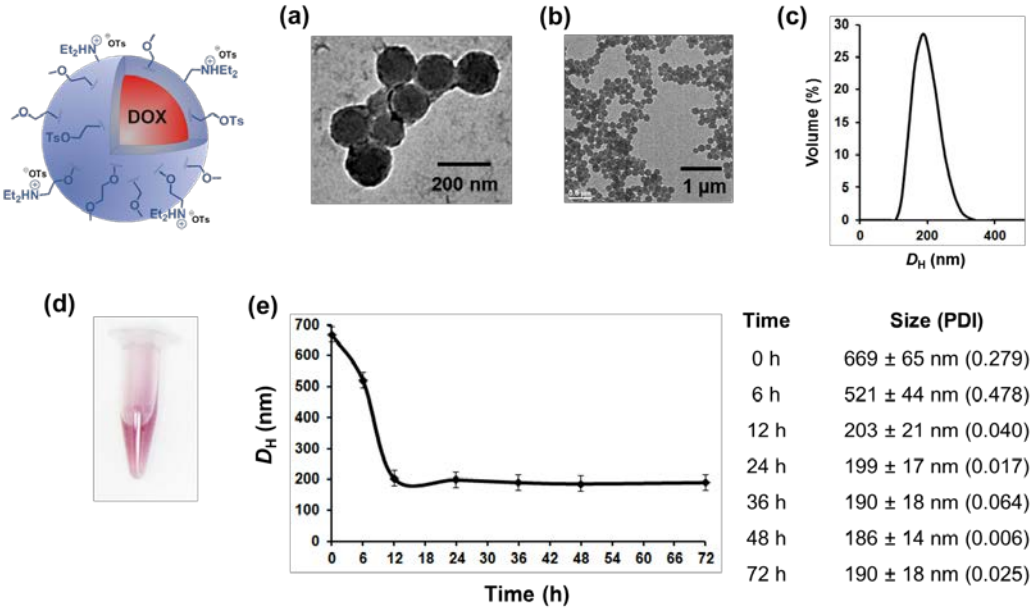

Fig. S15. A schematic representation of the $HNEt_2$-modified PNPs derived from copolymer (**2**-*co*-**4**)$_{15}$-*b*-**3**$_{15}$. (a) A representative TEM image of this material after being suspended in PBS (10 mM, pH 7.4, 150 mM [NaCl]), indicating a well-defined, narrowly dispersed spherical morphology; (b) a low-magnification TEM image of this material; (c) D_H distribution of these PNPs in PBS as measured by DLS; (d) a photograph of an aliquot of the PNPs re-suspended in PBS in an Eppendorf tube, clearly indicating retention of PNP dispersibility upon surface modification; and (e) DLS data showing the stabilization of $HNEt_2$-modified PNPs as a function of a time. PNPs are stabilized in PBS after a 12 h incubation period with $HNEt_2$.

Characterization of H_2NEt-modified PNPs and assessment of PNP dispersibility as a function of time. H_2NEt-modified PNPs retained the narrow size disribution of the parent PNPs (PDI = 0.053 with D_H = 190 ± 18 nm), as indicated by DLS and TEM (Fig. S16). To further probe the stabilization behavior over time, the PNP surface displacement reaction was monitored at 0, 6, 12, 24, 36, 48, and 72 h (Fig. S16e). Improved PNP dispersibility in PBS was observed after a period of 12 h, indicating that sufficient surface tosylate groups were displaced by H_2NEt to result in charge stabilization of the PNPs.

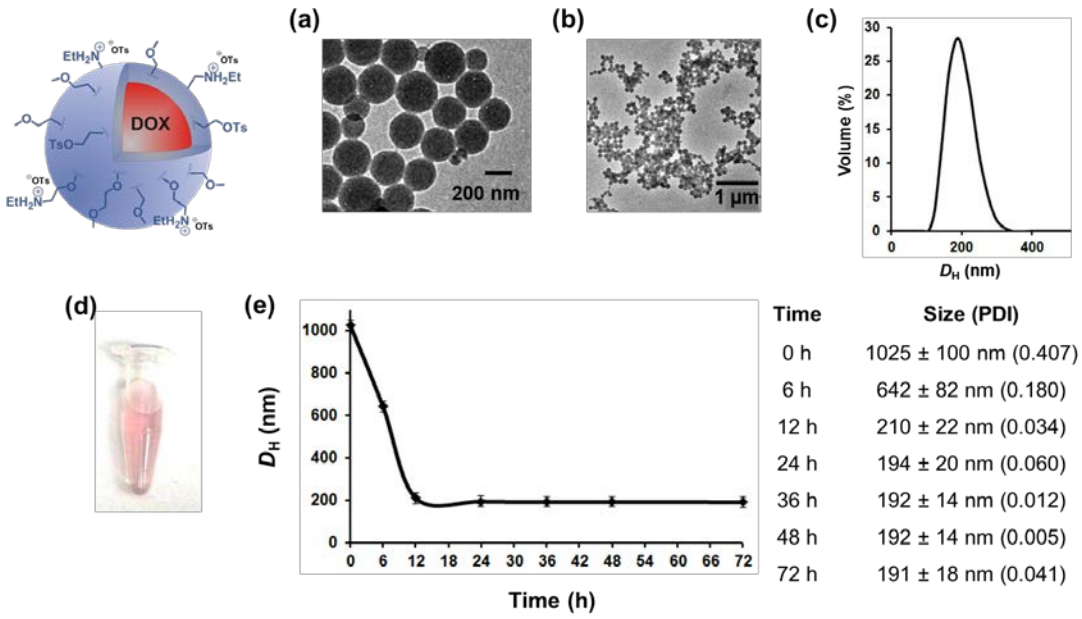

Fig. S16. A schematic representation of the H_2NEt-modified PNPs derived from copolymer (**2**-*co*-**4**)$_{15}$-*b*-**3**$_{15}$. (a) A representative TEM image of this material after being suspended in PBS (10 mM, pH 7.4, 150 mM [NaCl]), indicating a well-defined, narrowly dispersed spherical morphology; (b) a low-magnification TEM image of this material; (c) D_H distribution of these PNPs in PBS as measured by DLS; (d) a photograph of an aliquot of the PNPs re-suspended in PBS in an Eppendorf tube, clearly indicating retention of PNP dispersibility upon surface modification; and (e) DLS data showing the stabilization of H_2NEt-modified PNPs as a function of a time. PNPs are stabilized in PBS after a 12 h incubation period with H_2NEt.

Characterization of 2-methoxyethylamine-modified PNPs and assessment of PNP dispersibility as a function of time. 2-methoxyethylamine-modified PNPs retained the narrow size disribution of the parent PNPs (PDI = 0.053 with D_H = 190 ± 18 nm), as indicated by DLS and TEM (Fig. S17). To further probe the stabilization behavior over time, the PNP surface displacement reaction was monitored at 0, 6, 12, 24, 36, 48, and 72 h (Fig. S17e). Improved PNP dispersibility in PBS was observed after a period of 12 h, indicating that sufficient surface tosylate groups were displaced by 2-methoxyethylamine to result in charge stabilization of the PNPs.

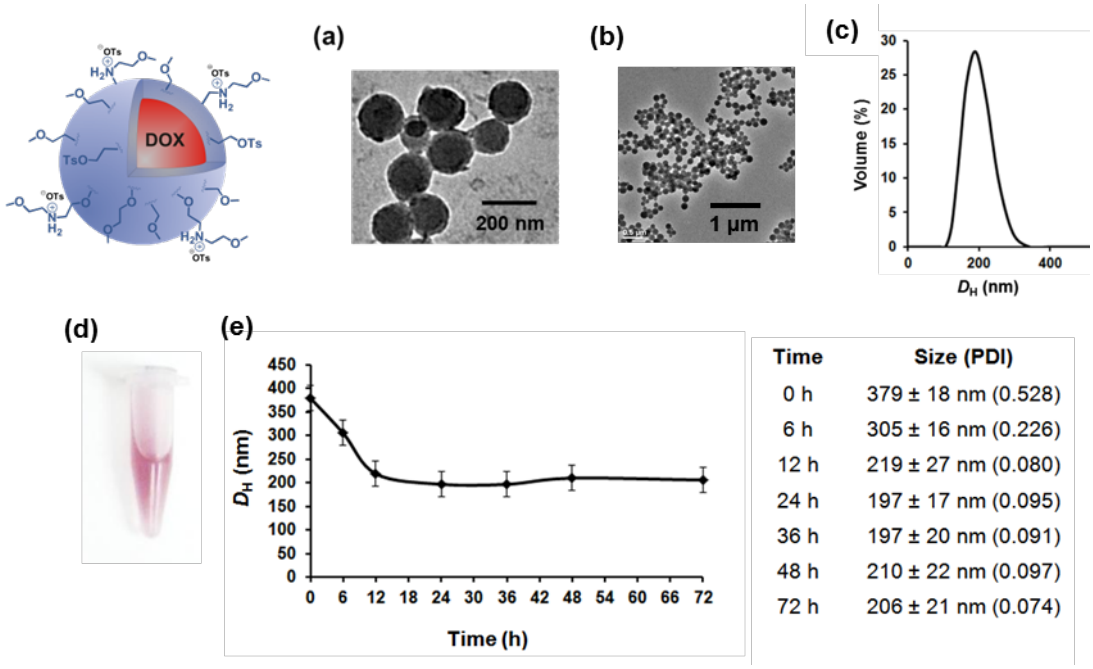

Fig. S17. A schematic representation of the 2-methoxyethylamine-modified PNPs derived from copolymer (**2**-*co*-**4**)$_{15}$-*b*-**3**$_{15}$. (a) A representative TEM image of this material after being suspended in PBS (10 mM, pH 7.4, 150 mM [NaCl]), indicating a well-defined, narrowly dispersed spherical morphology; (b) a low-magnification TEM image of this material; (c) D_H distribution of these PNPs in PBS as measured by DLS; (d) a photograph of an aliquot of the PNPs re-suspended in PBS in an Eppendorf tube, clearly indicating retention of PNP dispersibility upon surface modification; and (e) DLS data showing the stabilization of 2-methoxyethylamine-modified PNPs as a function of a time. PNPs are stabilized in PBS after a 12 h incubation period with 2-methoxyethylamine.

Characterization of 2-methylthioethylamine-modified PNPs and assessment of PNP dispersibility as a function of time. 2-methylthioethylamine-modified PNPs retained the narrow size disribution of the parent PNPs (PDI = 0.053 with D_H = 190 ± 18 nm), as indicated by DLS and TEM (Fig. S18). To further probe the stabilization behavior over time, the PNP surface displacement reaction was monitored at 0, 6, 12, 24, 36, 48, and 72 h (Fig. S18e). Improved PNP dispersibility in PBS was observed after a period of 12 h, indicating that sufficient surface tosylate groups were displaced by 2-methylthioethylamine to result in charge stabilization of the PNPs.

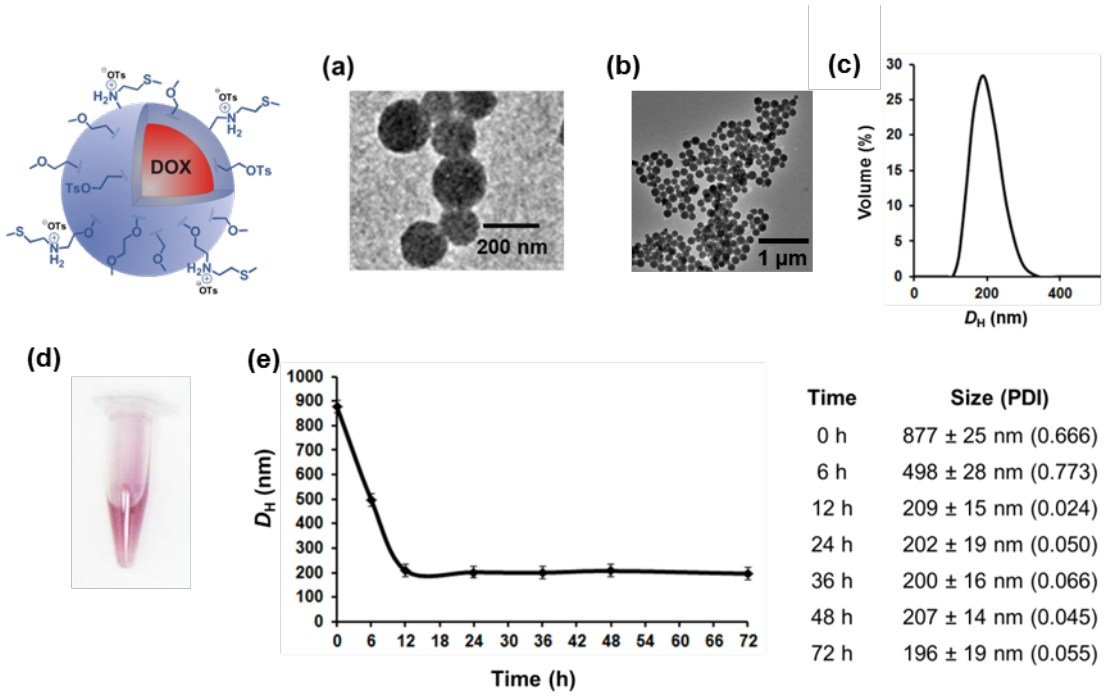

Fig. S18. A schematic representation of the 2-methylthioethylamine-modified PNPs derived from copolymer (**2**-*co*-**4**)$_{15}$-*b*-**3**$_{15}$. (a) A representative TEM image of this material after being suspended in PBS (10 mM, pH 7.4, 150 mM [NaCl]), indicating a well-defined, narrowly dispersed spherical morphology; (b) a low-magnification TEM image of this material; (c) D_H distribution of these PNPs in PBS as measured by DLS; (d) a photograph of an aliquot of the PNPs re-suspended in PBS in an Eppendorf tube, clearly indicating retention of PNP dispersibility upon surface modification; and (e) DLS data showing the stabilization of 2-methylthioethylamine-modified PNPs as a function of a time. PNPs are stabilized in PBS after a 12 h incubation period with 2-methylthioethylamine.

A potential concern with using primary and secondary amines to modify the tosyl-functionalized PNPs was that the surface ammonium groups could be neutralized by the excess amine in solution and react further with the other tosyl groups on the PNP surface, resulting in cross-linking of the polymer chains. To evaluate if such reaction has occurred, aliquots (1 mL) of the amine-modified PNPs (both primary and secondary) were centrifuged for 30 min at 10K rpm to solid pellets which were isolated from the supernatant and dissolved in HPLC-grade THF (1 mL). The resulting solutions were completely clear, suggesting that there were no insoluble materials. GPC analyses of these solutions reveal the presence of only monomodal polymers with no detectable change in molecular weights from the starting polymers (Fig. S19a H_2NEt-modified PNPs: M_n = 20000 (pre-modification M_n = 19000), PDI = 1.61; Fig. S19b $HNEt_2$-modified PNPs: M_n = 19000 (pre-modification M_n = 19000), PDI = 1.44). If there was any occurrence of cross-linking between the polymer chains within a PNP, we would not expect these monomodal molecular weight distributions. (The slight increases in PDI observed for the molecular weight distributions of the polymers in the dissolved PNPs can be attributed to the non-uniform tosylate displacement on the polymer chains).

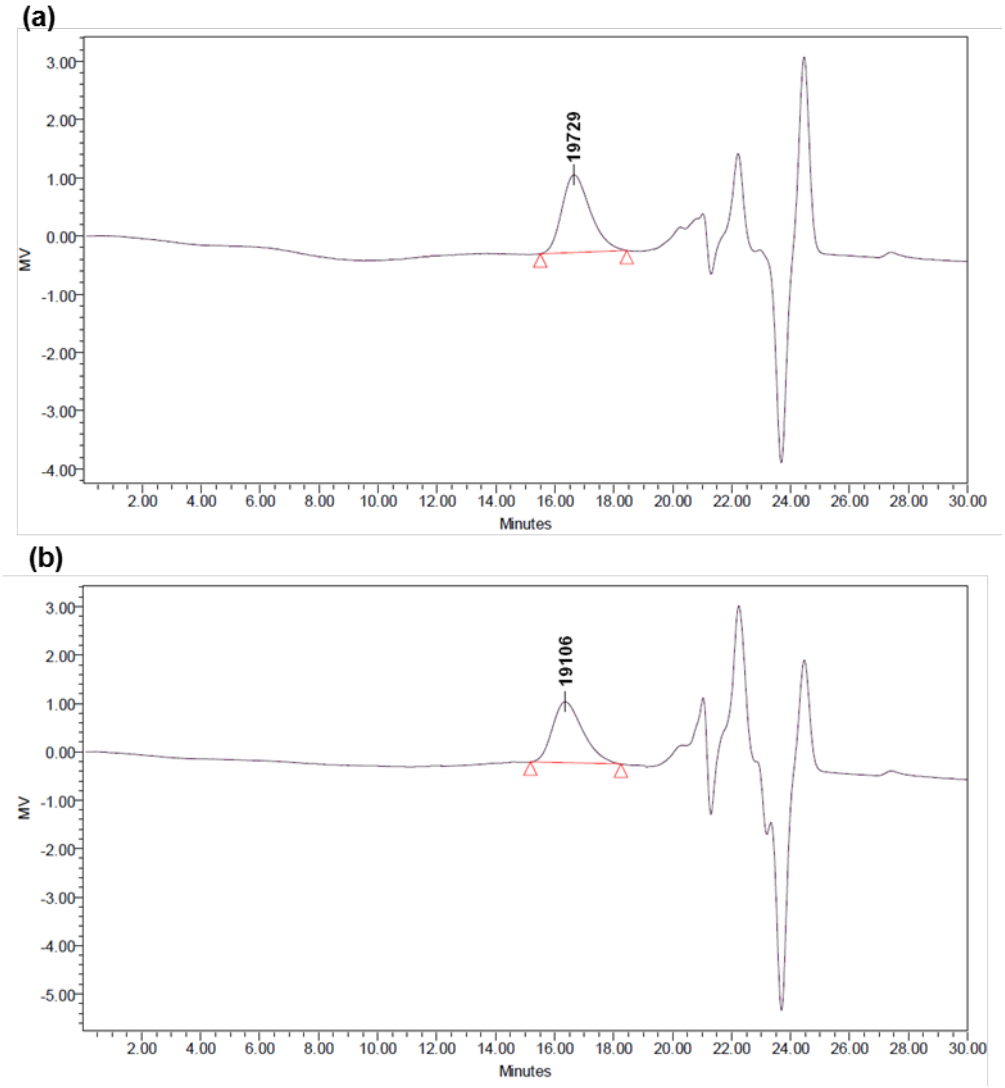

Fig. S19. Analytical GPC traces of the dissolved polymer chains from (a) H_2NEt- and (b) $HNEt_2$-modified PNPs derived from block copolymer (**2**-*co*-**4**)$_{15}$-*b*-**3**$_{15}$. A monomodal molecular weight distribution and retention of molecular weight of the parent polymer indicates that no further cross-linking reaction occurs on the PNP surface.

Quantification of amines on PNP surface subsequent to the tosylate displacement reaction. An aliquot of the PNPs (2.5 mL) derived from copolymer (**2**-*co*-**4**)$_{15}$-*b*-**3**$_{15}$ was transferred to a 1.5-mL safe-lock Eppendorf tube and incubated with alkyne-functionalized dimethylpropargylamine (dMPA), methylpropargylamine (MPA), or propargylamine (PA) following the procedure described in the Materials and methods section for "General procedure for tosylate displacement on PNPs" in the main manuscript. The alkyne-functionalized PNPs were then

centrifuged for 30 min at 10K rpm to a solid pellet, the supernatant was removed, and the PNPs were re-suspended in ultrapure deionized water (500 µL). An aliquot (2 mL) of the alkyne-functionalized dMPA-, MPA-, and PA-modified PNPs was subjected to "click" chemistry conditions in the presence of folate-PEG-azide as reported previously.[S3] Folate-modified PNPs retained the narrow size distribution of the parent PNPs (PDI = 0.071 with D_H = 188 ± 15 nm), as indicated by DLS and TEM (Fig. S20). To assess the degree of modification, a calibration curve of folic acid absorbance (ε = 27022 cm^{-1} M^{-1} at λ_{max} = 278 nm) in water was constructed with several folic acid concentrations (0, 0.005, 0.01, 0.025, 0.05 mmol/L). An aliquot (1 mL) of the purified folate-modified PNP suspension was pipetted into a 1-mL cuvette and its absorbance was recorded. The folate-conjugated dMPA-, MPA-, and PA-modified PNPs contained ~320, 650, and 1200 folate groups, respectively as determined by UV-vis spectroscopy. As expected, PNPs obtained from the control experiment (in the absence of $CuSO_4 \cdot 5H_2O$ and sodium ascorbate) showed no significant absorbance in the folate region.

To quantify the azide-alkyne coupling in a more accurate manner, the absorbance of an aliquot (500 µL) of folate-conjugated PNPs, that were lyophilized and re-dissolved in DMSO, was measured. Based on the calibration curve, it was determined that ~340, 655, and 1215 folate groups were coupled to the surface of dMPA-, MPA-, and PA-modified PNPs, respectively. Because the number of folate groups obtained by this method closely matched the number obtained for intact PNP (see previous paragraph), we decided to use these initially determined values directly.

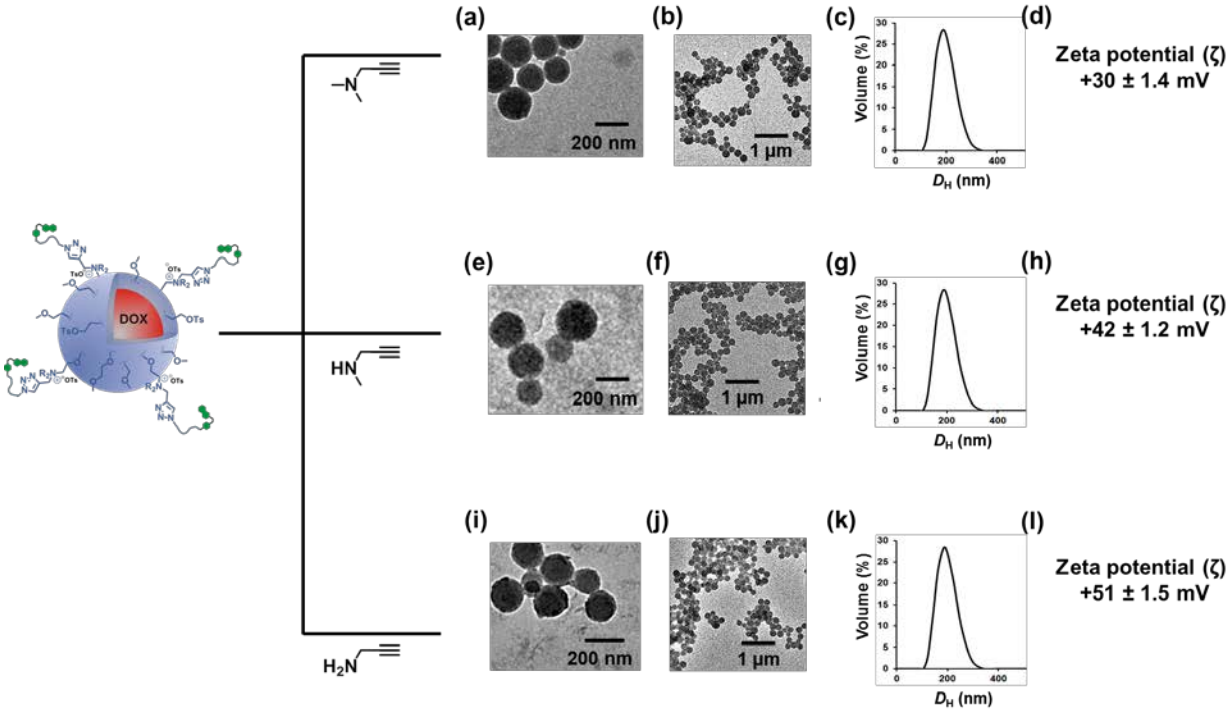

Fig. S20. Representative TEM images, D_H distributions, and zeta potentials (as measured by DLS) for folate-conjugated PNPs derived from dMPA-modified PNPs (a, b c, and d), MPA-modified PNPs (e, f, g, and h), and PA-modified PNPs (i, j, k and l). All three sets of data indicate retention of the original well-defined, narrowly dispersed spherical morphology.

Varying stoichiometric ratio of amine added to PNPs. Using a similar protocol as that specified in the Materials and methods section for "General procedure for tosylate displacement on PNPs" in the main manuscript, the minimum amount of amine required to stabilize the PNPs in PBS was determined by varying the stoichiometric ratio of amine added to the PNPs prior to incubation. The NEt_3- and $HNEt_2$-modified PNPs were successfully stabilized in PBS with the addition of NEt_3 (0.5 µL, 0.2 equiv with respect to the amount of tosylate groups) and $HNEt_2$ (0.5 µL, 0.3 equiv with respect to the amount of tosylate groups), respectively (Fig. S21a and S21b, respectively). On the other hand, 8 equiv each of H_2NEt, 2-methoxyethylamine, or 2-methylthioethylamine were required to stabilize the PNPs in PBS (Fig. S21c, S21d, and S21e, respectively).

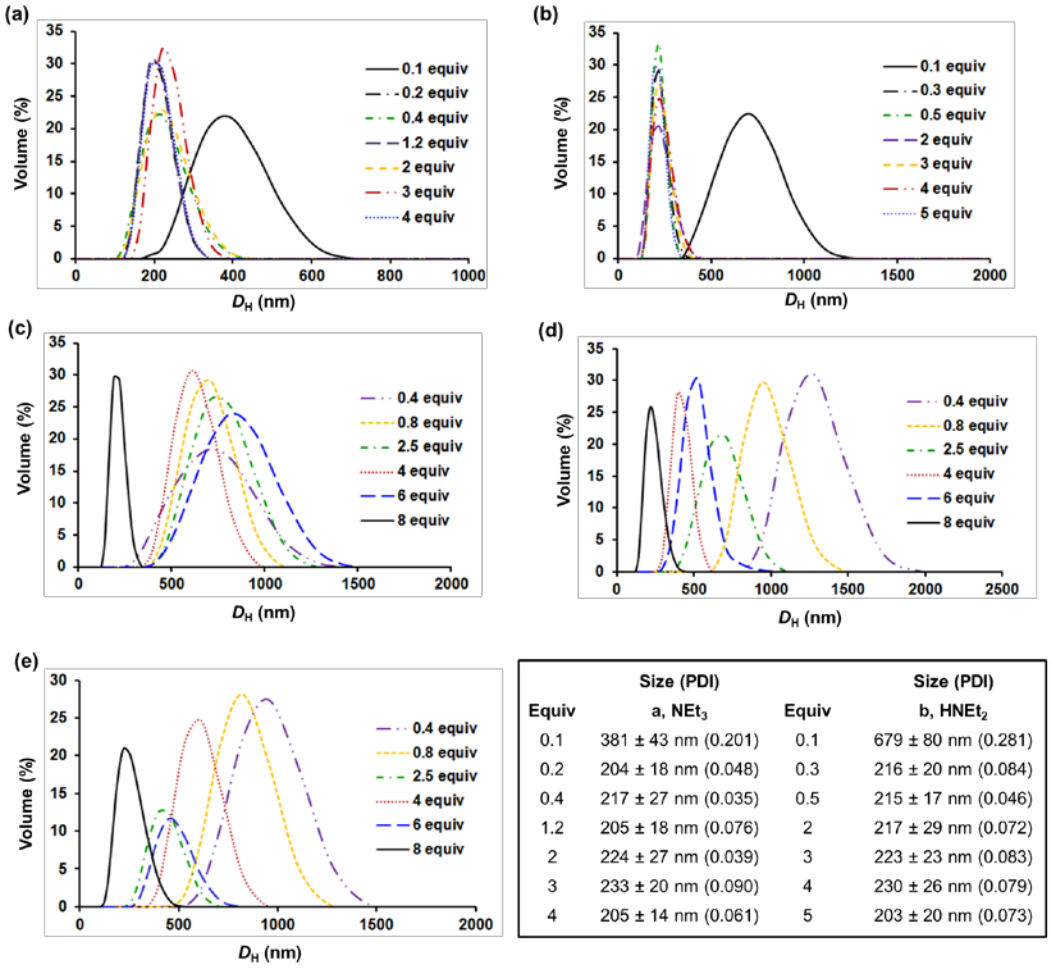

Equiv	Size (PDI) a, NEt_3	Equiv	Size (PDI) b, $HNEt_2$
0.1	381 ± 43 nm (0.201)	0.1	679 ± 80 nm (0.281)
0.2	204 ± 18 nm (0.048)	0.3	216 ± 20 nm (0.084)
0.4	217 ± 27 nm (0.035)	0.5	215 ± 17 nm (0.046)
1.2	205 ± 18 nm (0.076)	2	217 ± 29 nm (0.072)
2	224 ± 27 nm (0.039)	3	223 ± 23 nm (0.083)
3	233 ± 20 nm (0.090)	4	230 ± 26 nm (0.079)
4	205 ± 14 nm (0.061)	5	203 ± 20 nm (0.073)

Equiv	Size (PDI) c, H_2NEt	d, 2-methoxyethylamine	e, 2-methylthioethylamine
0.4	679 ± 100 nm (0.212)	1420 ± 130 nm (0.806)	933 ± 80 nm (0.636)
0.8	679 ± 43 nm (0.167)	959 ± 70 nm (0.753)	814 ± 67 nm (0.720)
2.5	743 ± 75 nm (0.162)	666 ± 63 nm (0.583)	424 ± 40 nm (0.493)
4	613 ± 55 nm (0.211)	413 ± 29 nm (0.462)	593 ± 51 nm (0.624)
6	816 ± 93 nm (0.169)	491 ± 28 nm (0.581)	466 ± 44 nm (0.580)
8	210 ± 22 nm (0.024)	230 ± 25 nm (0.080)	215 ± 32 nm (0.074)

Fig. S21. DLS data of (a) NEt_3-modified PNPs, (b) $HNEt_2$-modified PNPs, (c) H_2NEt-modified PNPs, (d) 2-methoxyethylamine-modified PNPs, and (e) 2-methylthioethylamine-modified PNPs derived from block copolymer (**2**-*co*-**4**)$_{15}$-*b*-**3**$_{15}$ suspended in PBS (10 mM, pH 7.4, 150 mM [NaCl]) using different stoichiometric ratios of the corresponding amine.

Monitoring the stability of charge-stabilized PNPs in PBS. To evaluate the dispersibility of charge-stabilized PNPs *in vitro*, we monitored their size distributions in PBS solutions. An aliquot of charge-stabilized PNPs (500 µL) in water was transferred to a 1.5-mL safe-lock Eppendorf tube and centrifuged for 30 min at 10K rpm to a solid pellet. The supernatant was removed and the PNPs were re-suspended in PBS (500 µL, 10 mM, pH = 8.5, [NaCl] = 150 mM). The size distribution of the charge-stabilized PNPs was determined using DLS over a period of 96 h. Within 3 h, aggregation was clearly observed for the NEt_3-modified PNPs (Fig. S22a) and the $HNEt_2$-modified PNPs (Fig. S22b), suggesting that these formulations were not able to render the PNPs stable in PBS solutions. In contrast, H_2NEt-modified PNPs (Fig. S22c), 2-methoxyethylamine-modified PNPs (Fig. S22d), and 2-methylthioethylamine-modified PNPs (Fig. S22e) maintained their narrow size distributions over this whole time period, indicating a high degree of dispersibility in PBS.

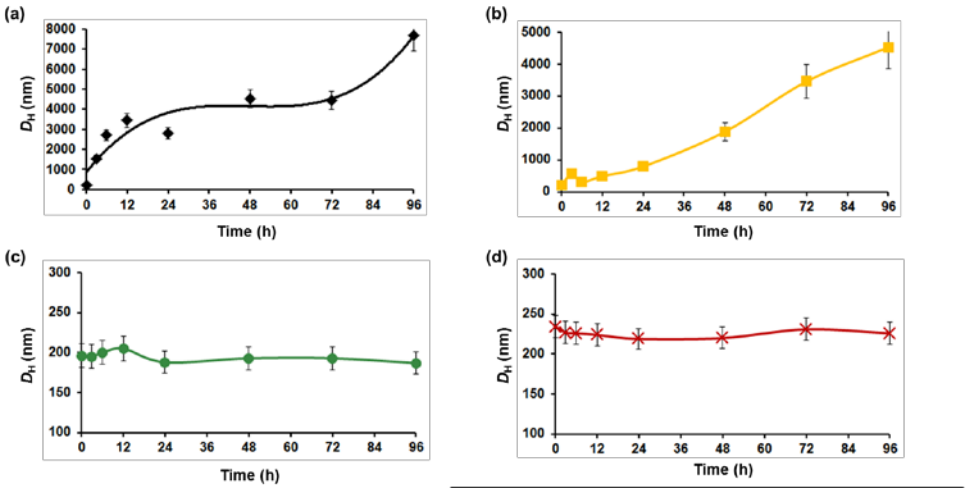

Time	Size (PDI) a, NEt_3	b, $HNEt_2$
0 h	204 ± 13 nm (0.036)	211 ± 11 nm (0.028)
3 h	1546 ± 62 nm (1.000)	568 ± 53 nm (0.615)
6 h	2710 ± 49 nm (1.000)	316 ± 75 nm (0.418)
12 h	3448 ± 62 nm (1.000)	496 ± 70 nm (0.528)
24 h	2817 ± 216 nm (1.000)	799 ± 63 nm (0.793)
48 h	4545 ± 96 nm (1.000)	1887 ± 96 nm (1.000)
72 h	4447 ± 757 nm (0.794)	3462 ± 38 nm (1.000)
96 h	7675 ± 456 nm (1.000)	4652 ± 115 nm (0.707)

Time	Size (PDI) c, H_2NEt	d, 2-methoxyethylamine	e, 2-methylthioethylamine
0 h	198 ± 15 nm (0.054)	234 ± 17 nm (0.003)	224 ± 16 nm (0.016)
3 h	196 ± 15 nm (0.061)	227 ± 18 nm (0.028)	225 ± 16 nm (0.022)
6 h	201 ± 14 nm (0.027)	226 ± 21 nm (0.072)	226 ± 16 nm (0.049)
12 h	206 ± 12 nm (0.071)	224 ± 17 nm (0.087)	224 ± 19 nm (0.013)
24 h	191 ± 13 nm (0.029)	219 ± 20 nm (0.084)	228 ± 16 nm (0.045)
48 h	193 ± 17 nm (0.007)	220 ± 20 nm (0.097)	225 ± 17 nm (0.011)
72 h	193 ± 14 nm (0.002)	231 ± 31 nm (0.088)	216 ± 20 nm (0.094)
96 h	190 ± 17 nm (0.054)	226 ± 20 nm (0.054)	218 ± 22 nm (0.052)

Fig. S22. DLS data of (a) NEt_3-modified PNPs and (b) $HNEt_2$-modified PNPs in PBS as a function of a time, clearly indicating that PNPs started to aggregate after 3 h; (c) H_2NEt-modified PNPs, (d) 2-methoxyethylamine-modified PNPs, and (e) 2-methylthioethylamine-modified PNPs in PBS as a function of a time, clearly indicating that these PNPs possess a high degree of stability even after a 96 h period.

Monitoring the release of doxorubicin from PNPs derived from block copolymer (2-*co*-4)$_{15}$-*b*-3$_{15}$. An aliquot of PNPs (500 µL) derived from block copolymer (**2**-*co*-**4**)$_{15}$-*b*-**3**$_{15}$ was transferred to a 1.5-mL Protein LoBind Eppendorf tube and centrifuged for 30 min at 10K rpm. The supernatant was removed and the absorbance at 480 nm was measured using UV-vis spectroscopy. The supernatant was then replaced with acidified ultrapure deionized water (500 µL, pH 5 as adjusted with the addition of aq. HCl) and the tube was placed on a platform shaker. The absorbance of the supernatant at 480 nm was measured at different time points over a period of 48 h. The theoretical molecular weight of the polymer was used to determine the concentration of doxorubicin at 100% release from the copolymer (Fig. S23a). As doxorubicin is released from the PNPs, we expect the spherical PNPs to collapse and affect the size distribution. Monitoring the size distribution of PNPs post-drug release using DLS analysis supported our conjecture (Fig. S23b).

While the doxorubicin release profile shown in Fig. 23a may appear to be surprising at first, it compares well to that demonstrated in our previous work[S4] for a methoxy-functionalized, doxorubicin-containing PNP platform at pH 4. In addition, doxorubicin has been conjugated to a variety of polymer systems [S5-S7] through carbamate linkages resulting in materials with similar drug release profiles as ours at pH 5. Our hypotheses for the slow drug release rate after the 12 h period are:

- As the drug is released during the initial time period, the PNPs begin to aggregate (as evidenced by DLS, Fig. S23b). Such aggregation results in a different PNP morphology, changing the overall drug release rate midway.
- The PNPs may in fact possess an onion-shell type of morphology, where hydrophobic layers alternates with hydrophilic ones,[S8] instead of a core-shell structure where the core is hydrophobic and the shell is hydrophilic. Such a morphology would significantly affect the drug release rate after the drug has been released from the first few layers: the outer hydrophobic layers would release the drug quickly; however, the inner hydrophobic layers would release the drug at a much slower rate.

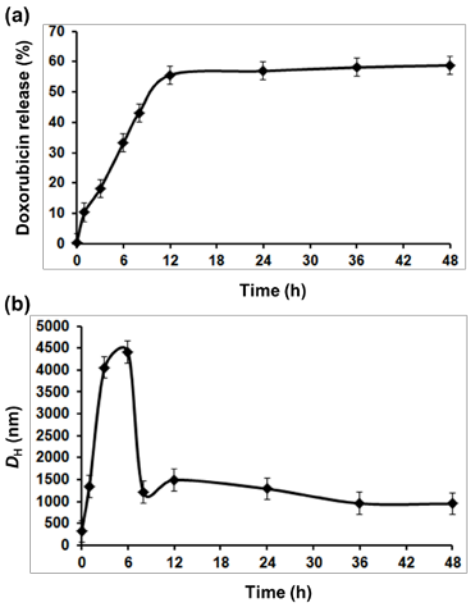

Time	Drug release (%)
0 h	0.3 ± 0.4
3 h	10.3 ± 1.2
6 h	18.1 ± 1.4
8 h	33.2 ± 1.3
12 h	43.1 ± 1.6
24 h	55.6 ± 1.9
36 h	58.1 ± 1.8
48 h	58.8 ± 2.3

Time	Size (PDI)
0 h	315 ± 32 (0.023)
1 h	1345 ± 87 (0.528)
3 h	4059 ± 85 (1.000)
6 h	4410 ± 216 (1.000)
8 h	1215 ± 76 (0.692)
12 h	1492 ± 77 (0.515)
24 h	1288 ± 67 (0.409)
36 h	955 ± 51 (1.000)
48 h	950 ± 52 (0.839)

Fig. S23. (a) Release profile of doxorubicin from PNPs derived from copolymer (**2**-*co*-**4**)$_{15}$-*b*-**3**$_{15}$ at pH 5. Data were collected over a 48 h period. (b) DLS data of these PNPs after being exposed to pH 5 water, indicating aggregation of PNPs upon release of doxorubicin over a 48 h period.

VI. Synthesis of cholesterol-containing block copolymer (2-*co*-4)$_{15}$-*b*-8$_{15}$, its PNP formation, and surface modification *via* tosylate displacement.

3-((4-((1*S*,2*S*,4*S*)-bicyclo[2.2.1]hept-5-en-2-yloxy)benzyl)oxy)-10,13-dimethyl-17-(6-methylheptan-2-yl)-2,3,4,7,8,9,10,11,12,13,14,15,16,17-tetradecahydro-1*H*-cyclopentaphenanthrene (**8**) and block copolymer **2**$_{15}$-*b*-**8**$_{15}$ were prepared following a previously published protocol.[S9]

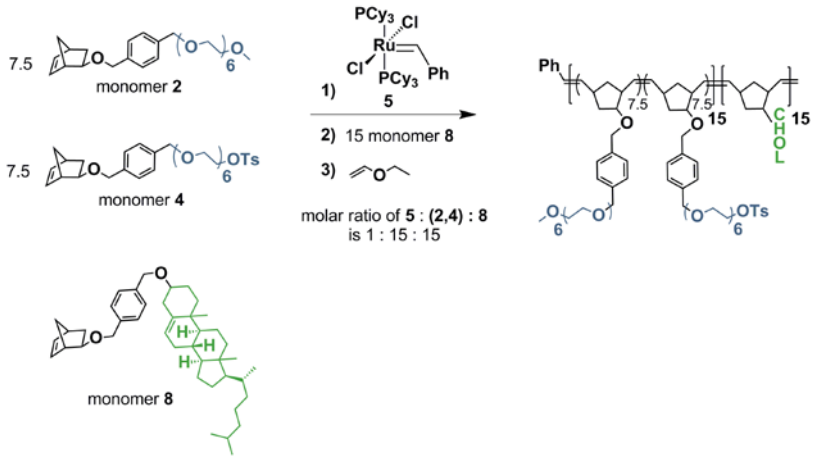

Synthesis of block copolymer (2-*co*-4)$_{15}$-*b*-8$_{15}$. In an inert-atmosphere glovebox, monomers **2** (11.8 mg, 0.0231 mmol) and **4** (15 mg, 0.0231 mmol) were dissolved together in anhydrous THF (2 mL) in a 20-mL scintillation vial equipped with a magnetic stirring bar. A stock solution of catalyst **5** (5 mg) in THF (5 mL) was prepared, a portion of which (2.54 mL, 3.08 μmol) was added to the vial containing the mixture of monomers **2** and **4** under vigorous stirring. The resulting reaction mixture was stirred at room temperature for 30 min, at which time an aliquot (100 μL) was removed and quenched with excess ethyl vinyl ether. A portion of this quenched aliquot was evaporated to dryness, redissolved in $CDCl_3$, and analyzed by ^{1}H NMR spectroscopy, which indicated complete consumption of the monomer. The remaining portion was evaporated to dryness, dissolved in HPLC-grade THF, and subjected to GPC analysis (M_n = 10000 (theoretical M_n = 9000), PDI = 1.17).

Immediately after aliquot removal, a solution of monomer **8** (27.7 mg, 0.0447 mmol) in THF (1.5 mL) was added to the reaction vial and the resulting polymerization mixture was stirred for an additional 30 min before being terminated with the addition of ethyl vinyl ether (1 mL). The reaction mixture was then added quickly into vigorously stirred cold (-10 °C) pentanes (200 mL), and the resulting precipitate was isolated *via* vacuum filtration and washed thoroughly with fresh pentanes to afford the product copolymer quantitatively as a light yellow solid. ^{1}H NMR ($CDCl_3$, Fig. S24): δ 0.77 (bs), 1.08 (bs), 1.25 (bd), 1.35 (bs), 1.41 (bs), 1.81 (bm), 2.25 (bs), 2.45 (bs), 2.53 (bd), 2.86-3.30 (bm), 3.55-3.94 (bm), 4.15 (bs), 4.37-4.64 (bm), 5.12-5.56 (bm), 7.22-7.61 (bm), 7.79 (bd), 7.96 (bd). GPC: M_n = 19000 (theoretical M_n = 19000), PDI = 1.13.

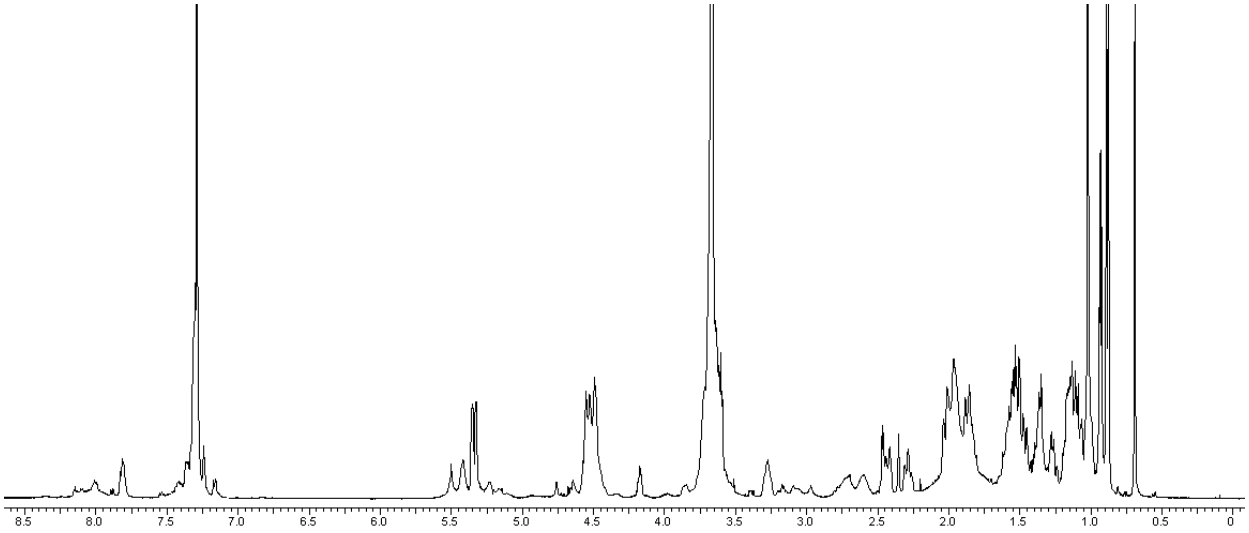

Fig. S24. The ^{1}H NMR spectrum of block copolymer (**2**-*co*-**4**)$_{15}$-*b*-**8**$_{15}$.

General procedure for the preparation of nanoparticle dispersions. The block copolymer (**2**-*co*-**4**)$_{15}$-*b*-**8**$_{15}$ was first dissolved in THF prior to the preparation of polymer nanoparticles, following a similar protocol as described in the Materials and methods section, "General procedure for the preparation of nanoparticle dispersions" subsection, in the main manuscript. DLS analysis of the final PNP aqueous suspension revealed narrowly dispersed PNPs with an average diameter (D_H) of 200 ± 20 nm and a corresponding PDI of 0.074 (Fig. S25c). TEM analysis indicated a uniform size distribution for the PNPs in the solid state, with an average diameter of ~200 nm (Fig. S25a) that is consistent with the DLS data. An aliquot of the PNPs (500 µL) was transferred to a 1.5-mL safe-lock Eppendorf tube and lyophilized to a solid pellet. The dried PNPs were re-suspended in PBS (500 µL, 10 mM, pH = 8.5, [NaCl] = 150 mM). The PNPs that have been suspended in PBS shows a well-defined spherical morphology that is comparable to that of the parent PNPs, as observed by TEM and DLS (Fig. S25d and S25f: D_H = 190 ± 15 nm, PDI = 0.065).

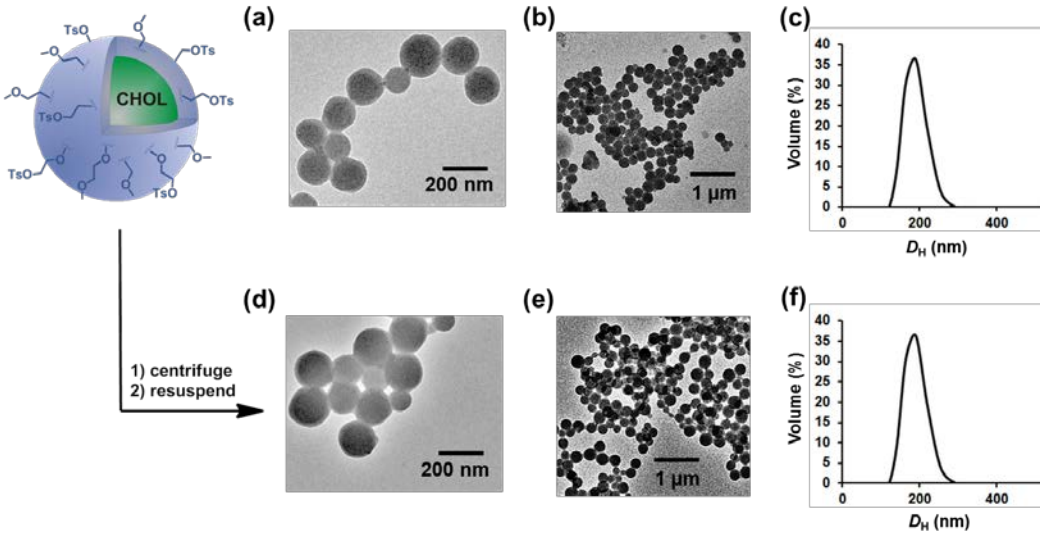

Fig. S25. Left: A schematic representation of the PNPs derived from block copolymer (**2**-*co*-**4**)$_{15}$-*b*-**8**$_{15}$. Right top panels: (a) a representative TEM image of these PNPs in ultrapure deionized water; (b) a low-magnification TEM image of this material; and (c) the corresponding D_H distribution of these PNPs as measured by DLS. Right bottom panels: (d) a representative TEM image of these PNPs upon centrifugation and resuspension in PBS (10 mM, pH 7.4, 150 mM [NaCl]); (e) a low-magnification TEM image of this material; and (f) the corresponding D_H distribution of these PNPs, clearly showing the retention of the original narrowly dispersed suspension.

Surface modification of tosyl-functionalized cholesterol-containing PNPs. An aliquot of the PNPs (500 μL) derived from copolymer (**2**-*co*-**4**)$_{15}$-*b*-**8**$_{15}$ was transferred to a 1.5-mL safe-lock Eppendorf tube and incubated with NEt_3, $HNEt_2$, H_2NEt, 2-methoxyethylamine, or 2-methylthioethylamine following the procedure outlined in the Materials and methods section "General procedure for tosylate displacement on PNPs" in the main manuscript. DLS data of these surface-modified PNPs in ultrapure deionized water are listed in Table S1.

Table S1. DLS data of charge-stabilized cholesterol-containing PNPs derived from copolymer (**2**-*co*-**4**)$_{15}$-*b*-**8**$_{15}$ in ultrapure deionized water.

Modified PNP	Size (PDI)
NEt_3-modified	213 ± 30 (0.098)
$HNEt_2$-modified	195 ± 18 (0.018)
H_2NEt-modified	211 ± 18 (0.037)
2-methoxyethylamine-modified	207 ± 22 (0.071)
2-methylthioethylamine-modified	214 ± 43 (0.103)

VII. MTS assay and confocal laser scanning microscopy.

MTS assay. To evaluate the inhibitory effects of the charge-stabilized PNPs, MDA-MB-231-Br cells (1.5×10^4 cells/mL) were seeded in 96-well tissue culture plates (Grenier Bio One North America, Monroe, NC, USA) for 24 h prior to drug treatment. The adhered cells were then incubated with serial dilutions of the cholesterol- and

doxorubicin-containing PNPs for 72 h, starting at 100 µM cholesterol and doxorubicin. After treatment, relative cell viability was determined using CellTiter 96 AQueous Non-Radioactive Cell Proliferation (MTS) Assay (Promega Corporation, Madison, WI, USA). The data was fitted to a model of dose-dependent inhibition of growth (GraphPad Prism, GraphPad Software, Inc., La Jolla, CA).

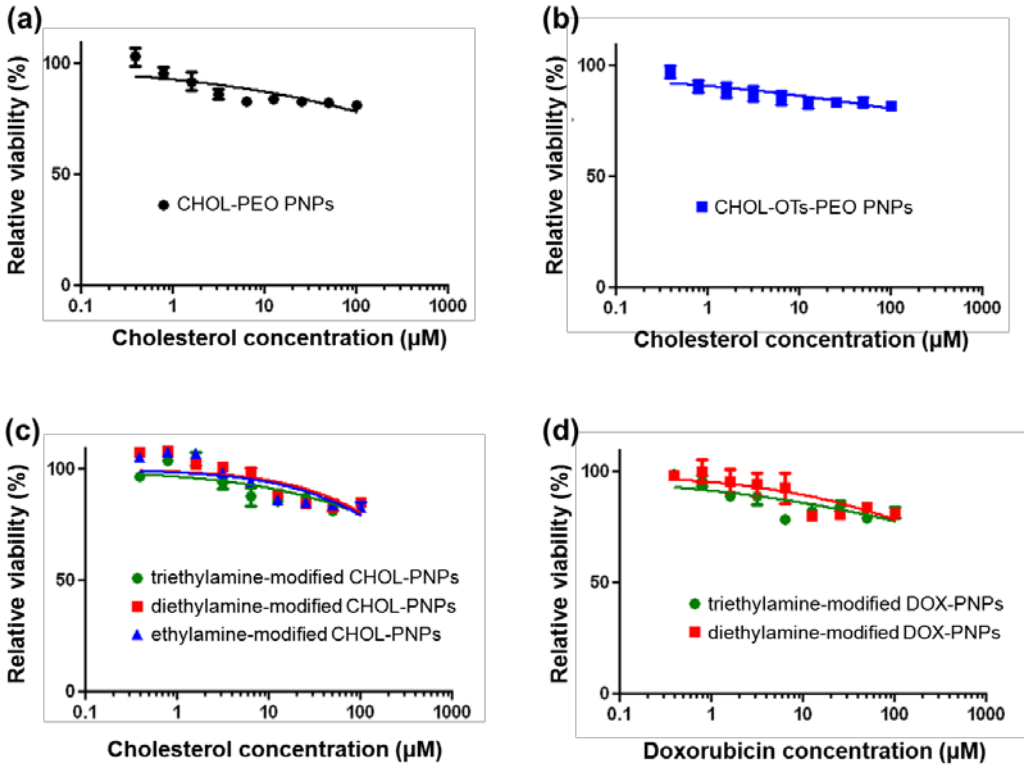

Fig. S26. In vitro cytotoxicity profiles of : (a) tosyl-functionalized cholesterol-containing PNPs, (b) methoxy-terminated cholesterol-contaning PNPs, (c) NEt_3-, $HNEt_2$-, and H_2NEt-modified cholesterol-containing PNPs, and (d) NEt_3- and $HNEt_2$-modified doxorubicin-containing PNPs. None of these PNPs exhibit any significant cytotoxic effect at the tested concentrations, indicating that doxorubicin was the active agent responsible for the observed cytotoxic response.

Confocal laser scanning microscopy studies. Non-green fluorescent protein (GFP)-producing MDA-MB-231-Br cells were plated in FluoroDish cell culture dish (World Precision Instruments, Sarasota, FL, USA; 500 kcell/mL) for 24 h at 37 °C and 5% (v/v) CO_2 before each experiment. Each dish was then incubated with the appropriate drug formulation for 4 h at 37 °C and 5% (v/v) CO_2. The drug-containing medium was then removed and the cell layers were washed with PBS (3 × 2 mL). CLSM images were then observed with inverted confocal laser scanning microscope (Carl Zeiss LSM 510 META) with excitation at 488 nm. At this wavelength, no observable background fluorescence was detected from the cell lines (Fig. S27a). A water-immersion objective, C-Apochromat 40X/1.20 W korr. UV-vis IR M27 was used. Obtained images were converted to TIFF format by using ZEN 2007 Light Edition SP1 software (Carl Zeiss).

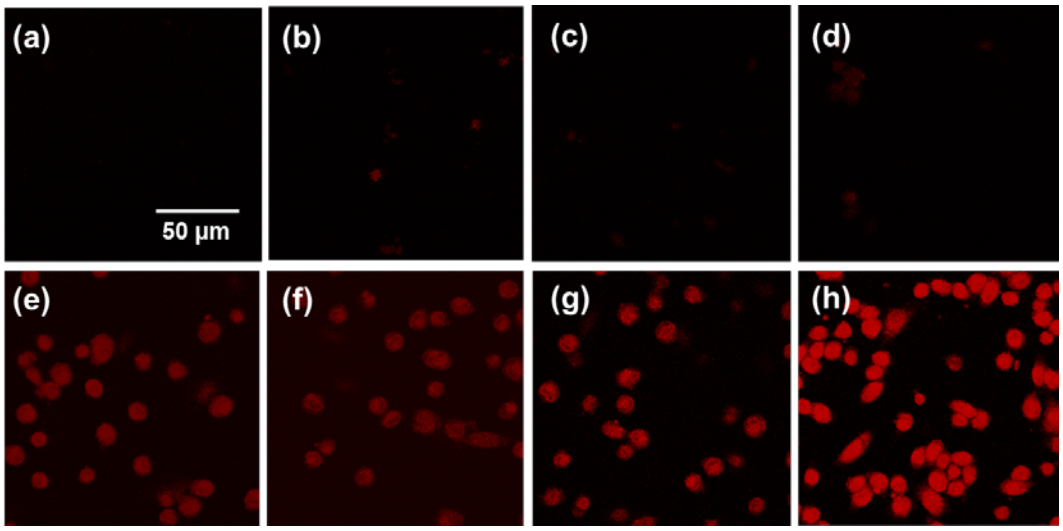

Fig. S27. Confocal laser-scanning fluorescence microscopy images, based on the fluorescence of doxorubicin, of (a) blank MDA-MB-231-Br cells and (b-h) of MDA-MB-231-Br cells after 4 h incubation with various doxorubicin-containing formulations: (b) tosyl-functionalized PNPs, (c) NEt_3-modified PNPs, (d) $HNEt_2$-modified PNPs, (e) H_2NEt-modified PNPs, (f) 2-methoxyethylamine-modified PNPs, (g) 2-methylthioethylamine, and (h) free doxorubicin. The high intensity of fluorescence in (h) can be attributed to the small-molecule nature of the free drug which allows it to freely diffuse into the cell. As a result, this image cannot be compared directly to those for the different PNP formulations, which are presumably localized at the cells through macromolecular transport pathways. (Exposure dose = 25 µM of doxorubicin).

VIII. Author contributions audit. S.A.K. and S.T.N. conceived the experiments presented herein. S.A.K. synthesized and characterized the monomers, polymers, and nanoparticles and performed the subsequent PNP functionalization experiments. E.P.S. carried out the *in vitro* MTS assay and confocal laser-scanning microscopy studies. T.V.O. supervised E.P.S. and S.T.N. supervised the project. S.A.K. wrote the initial draft of the paper with inputs from E.P.S. S.A.K. and S.T.N. finalized the manuscript.

IX. References:

S1. A. B. Pangborn, M. A. Giardello, R. H. Grubbs, R. K. Rosen and F. J. Timmers, *Organometallics*, 1996, **15**, 1518-1520.

S2. P. A. Bertin, J. M. Gibbs, C. K.-F. Shen, C. S. Thaxton, W. A. Russin, C. A. Mirkin and S. T. Nguyen, *J. Am. Chem. Soc.*, 2006, **128**, 4168-4169.

S3. S. A. Krovi, D. Smith and S. T. Nguyen, *Chem. Commun.*, 2010, **46**, 5277-5279.

S4. P. A. Bertin, PhD Thesis, Northwestern University, Evanston, IL, USA, 2005.

S5. B.-S. Kim, H.-i. Lee, Y. Min, Z. Poon and P. T. Hammond, *Chem. Commun.*, 2009, 4194-4196.

S6. X. Hu, S. Liu, Y. Huang, X. Chen and X. Jing, *Biomacromolecules*, 2010, **11**, 2094-2102.

S7. T. Liu, X. Li, Y. Qian, X. Hu and S. Liu, *Biomaterials*, 2012, **33**, 2521-2531.

S8. G. Battaglia and A. J. Ryan, *Macromolecules*, 2006, **39**, 798-805.

S9. D. Smith, S. H. Clark, P. A. Bertin, B. L. Mirkin and S. T. Nguyen, *J. Mater. Chem.*, 2009, **19**, 2159-2165.